

Transition Rates for a Rydberg Atom Surrounded by a Plasma

Chengliang Lin, Christian Gocke and Gerd Röpke

Universität Rostock, Institut für Physik, 18051 Rostock, Germany

Heidi Reinholz

Universität Rostock, Institut für Physik, 18051 Rostock, Germany and

University of Western Australia School of Physics, WA 6009 Crawley, Australia

(Dated: January 19, 2016)

We derive a quantum master equation for an atom coupled to a heat bath represented by a charged particle many-body environment. In Born-Markov approximation, the influence of the plasma environment on the reduced system is described by the dynamical structure factor. Expressions for the profiles of spectral lines are obtained. Wave packets are introduced as robust states allowing for a quasi-classical description of Rydberg electrons. Transition rates for highly excited Rydberg levels are investigated. A circular-orbit wave packet approach has been applied, in order to describe the localization of electrons within Rydberg states. The calculated transition rates are in a good agreement with experimental data.

PACS number(s): 03.65.Yz, 32.70.Jz, 32.80.Ee, 52.25.Tx

I. INTRODUCTION

Open quantum systems have been a fascinating area of research because of its ability to describe the transition from the microscopic to the macroscopic world. The appearance of the classicality in a quantum system, i.e. the loss of quantum informations of a quantum system can be described by decoherence resulting from the interaction of an open quantum system with its surroundings [1, 2].

An interesting example for an open quantum system interacting with a plasma environment are highly excited atoms, so-called Rydberg states, characterized by a large main quantum number. Rydberg states play an important role in astrophysics to study stellar atmospheres [3, 4]. Particularly, ionization processes of Rydberg states of hydrogen and helium and their recombination processes are significant for hydrogen and helium plasmas in a very low-density environment which exists in stellar atmospheres with weakly ionized layers [3, 5, 6]. Because the interaction with the plasma, characterized by the plasma frequency, is no longer small compared to the energy differences of quantum eigenstates, the surrounding plasma cannot be considered as a weak perturbation of the excited atom. The time evolution, in particular transition rates, is modified as shown in this work. An essential problem is the construction of optimum, robust states.

Note that Rydberg states are energetically near to the continuum of scattering states. The screening of a given ion by the free electrons and neighboring ions in a plasma results in the reduction of the ionization potential and line broadening of eigenenergy levels of the given atom. For the Rydberg states near the continuum edge, it may be quite difficult to rigorously distinguish the borderline between the real continuum edge and bound states. For example, it is known that in solar astrophysics spectral lines are visible up to main quantum numbers of about 17 [7]. The correct treatment of the Rydberg states which are near the continuum edge is a long-standing problem in plasma spectroscopy, see Refs. [8, 9]. Thus a many-body approach to Rydberg states in a plasma is also of interest for spectroscopy.

Because of their macroscopic characters and long lifetimes, nowadays Rydberg states become a fundamental concept of open quantum systems in different fields of physics, such as quantum information research [10–12] and ultracold plasmas [13–15]. Recently the existence of Rydberg excitons in the copper oxide Cu_2O [16] is demonstrated which enable visible measurements of coherent quantum effects [17]. Actually, using a localized semi-classical representation of bound states to study the connection between classical mechanics and the large-quantum number limit of quantum mechanics has been a topic of interest since the development of quantum mechanics [18, 19]. As a mesoscopic object, the Rydberg atom may be regarded as an outstanding example demonstrating both macroscopic classical and microscopic quantum behavior. In a series of papers of Stroud *et al.* [20–27], the dynamics of a hydrogenic Rydberg atom has been discussed in detail. It has been shown that the behavior of a wave packet constructed by energy eigenstates of the hydrogen atom is different for the short and the long-term evolution. This difference is essential for the investigation of the connection between the quantum and classical description of nature and gives a possibility to explain the emergence of classicality in a quantum system.

Motivated by these exciting perspectives, we study the properties of hydrogenic Rydberg atoms, in particular, the transition rates of highly excited Rydberg states. Different environments are of interest: the interaction with

the radiation field, the interaction with phonons (Rydberg excitons), the interaction with charged particles. We focus on the special case where the environment is described by a plasma background, see Refs. [28–30]. A similar derivation for a test particle interacting through collisions with a low-density background gas by using the quantum master equation approach is reported in Refs. [31, 32]. The influence of the plasma on the dynamics of the atom is determined by the dynamical structure factor of the surrounding plasma. Robust states are represented by optimized Gaussian wave packets. As an example, transition rates are calculated and compared to other theoretical approaches and experimental data.

Another example which will be considered are the profiles of spectral lines. They are essentially determined by the interaction of the bound states with the radiation field and the charge carriers of the plasma. Both of them can be treated as thermal bath for the bound states, which are regarded as the reduced system in the theory of open quantum systems. Various approaches can be used to calculate the spectral line profiles in a plasma environment, for instance, unified theory [33], quantum mechanical scattering theory [34] and the Green's function methods [35, 36], which are based on the assumption that the plasma is in equilibrium. Quantum kinetic theory, as a nonequilibrium approach, can also be applied to investigate the line profiles of the plasma which will be presented in this work.

This paper is organized as follows: in section II A we outline the derivation of the general quantum master equation in Born-Markov approximation. Then we discuss the special case of plasma as a many-body environment in Sec. II B. In Sec. II C, the general quantum master equation is investigated in detail by introducing the basis of the energy eigenstates of the hydrogen atom. The Pauli equation and the spectral line profiles are derived in this section. The wave packet description for the bound Rydberg electron is introduced in Sec. III. The robustness and validity of the wave packet description are discussed in Sec. III A. The transition rates for the hydrogenic Rydberg atom derived with the use of the circular-orbit wave packet and their comparisons with classical Monte-Carlo simulations and experimental data are presented in III B. Conclusions are drawn in Sec. IV.

II. QUANTUM MASTER EQUATION FOR RYDBERG ATOMS IN A PLASMA

A. General quantum master equation

We are investigating the reduced system of a Rydberg atom (A) embedded in a bath (B) consisting of charged particles c , electrons ($c = e$) and (singly) charged ions ($c = i$), charge e_c , mass m_c , particle density n_c and temperature T . The microscopic model under consideration is a hydrogen atom coupled to a surrounding charge-neutral plasma, $\sum_c e_c n_c = 0$. In the bath, in general, the formation of bound states such as atoms is also possible. Furthermore, the interaction of the atom is mediated by the Maxwell field which contains, besides the Coulomb interaction with the charged particles, also single-particle states, the photons. The total system is then described by the Hamiltonian

$$\hat{H} = \hat{H}_A + \hat{H}_B + \hat{H}_{\text{int}}. \quad (1)$$

In a plasma environment the Hamiltonian \hat{H}_B includes both the kinetic energy and the Coulomb interactions of charged particles \hat{H}_{Coul} (see Eq. (15) below) as well as the degrees of freedom of the photonic field $\hat{H}_{\text{photon}}^\perp$ describing the transversal Maxwell field of the plasma environment, i.e. $\hat{H}_B = \hat{H}_{\text{Coul}} + \hat{H}_{\text{photon}}^\perp$.

The atomic Hamiltonian reads in the non-relativistic case

$$\hat{H}_A = \frac{\hat{\mathbf{P}}^2}{2M} + \frac{\hat{\mathbf{p}}^2}{2m} - \frac{e^2}{4\pi\epsilon_0|\hat{\mathbf{r}}|}, \quad (2)$$

where the center-of-mass (c.o.m.) motion is described by the total mass $M = m_e + m_i$ and the variables $\hat{\mathbf{R}}, \hat{\mathbf{P}}$, the relative motion by the reduced mass m and the relative variables $\hat{\mathbf{r}}, \hat{\mathbf{p}}$. The eigenstates $|\Psi_{n,\mathbf{P}}\rangle$ of the isolated hydrogen atom are the solutions of the Schrödinger equation $\hat{H}_A|\Psi_{n,\mathbf{P}}\rangle = E_{n,\mathbf{P}}|\Psi_{n,\mathbf{P}}\rangle$ with the eigenenergy $E_{n,\mathbf{P}} = \mathbf{P}^2/(2M) + E_n$. The quantum number $n = \{\bar{n}, l, m, m_s\}$ describes the internal state for bound states $E_n < 0$ and $n = \{\mathbf{p}, m_s\}$ for scattering states $E_{\mathbf{p}} = \mathbf{p}^2/(2m) > 0$. For the bound states, the wave function $\Psi(\mathbf{R}, \mathbf{r}) = \langle \mathbf{R}, \mathbf{r} | \Psi_{n,\mathbf{P}} \rangle = \Psi_{\mathbf{P}}(\mathbf{R})\psi_n(\mathbf{r})$ contains the eigenstates $\psi_n(\mathbf{r})$ of the hydrogen atom. The c.o.m. motion $\Psi_{\mathbf{P}}(\mathbf{R})$ is given by a plane wave. In this work we concentrate on the internal degrees of freedom of the bound states. The c.o.m motion, which, e.g., determines the Doppler broadening of the spectral line profile, will not be discussed here in detail. In most cases it will be dropped considering the adiabatic limit.

The interaction between the atomic electron and the plasma environment is given by the coupling of the atomic current operator to the electromagnetic field of the bath

$$\hat{H}_{\text{int}}(t) = \int d^3\mathbf{r} \hat{j}_A^\mu(x) \hat{A}_{\mu,B}(x) \quad (3)$$

with $x^\mu = \{ct, \mathbf{r}\}$. Introducing the creation ($\hat{\psi}^\dagger(x)$) and annihilation ($\hat{\psi}(x)$) operator for the atomic electron, the current operator of the atomic subsystem $\hat{j}_A^\mu(x) = \{c\hat{\rho}_A(x), \hat{\mathbf{j}}_A(x)\}$ can be explicitly written as $\hat{\rho}_A(x) = -e\hat{\psi}^\dagger(x)\hat{\psi}(x)$ for the electron probability density and $\hat{\mathbf{j}}_A(x) = \frac{ie\hbar}{2m_e} \left[\hat{\psi}^\dagger(x) \frac{\partial}{\partial \mathbf{r}} \hat{\psi}(x) - \left(\frac{\partial}{\partial \mathbf{r}} \hat{\psi}^\dagger(x) \right) \hat{\psi}(x) \right]$ for the electric current density of the electron (non-relativistic limit). Without further explanation, the operators in this work are given in Heisenberg picture

$$\hat{O}(t) = e^{i\hat{H}t/\hbar} \hat{O} e^{-i\hat{H}t/\hbar}. \quad (4)$$

The source of the electromagnetic field of the bath $\hat{A}_B^\mu(x) = (\hat{U}_B(x), \hat{\mathbf{A}}_B(x))$ is the current density $\hat{j}_B^\mu(x)$ of all charge carriers in the plasma. In the present work the Coulomb gauge $\nabla \times \hat{\mathbf{A}}_B(x) = 0$ is used. The Fourier transform

$$\hat{\mathbf{j}}_{\mathbf{q},B}(\omega) = \int_{\Omega_0} d^3\mathbf{r} \int_{-\infty}^{\infty} dt e^{i\omega t - i\mathbf{q}\cdot\mathbf{r}} \hat{\mathbf{j}}_B(t, \mathbf{r}) \quad (5)$$

of the electrical current in the surrounding plasma can be decomposed into a transverse component $\sum_c \hat{\mathbf{j}}_{\mathbf{q},B}^{\perp,c}(\omega)$ coupled only to the vector potential $\hat{\mathbf{A}}_{\mathbf{q},B}(\omega)$ and a longitudinal one $\sum_c \hat{j}_{\mathbf{q},B}^{\parallel,c}(\omega) \mathbf{q}/q$ which is related only to the Coulomb potential. Because of the continuity equation, the relation $\mathbf{q} \cdot \hat{\mathbf{j}}_{\mathbf{q},B}(\omega) = q \hat{j}_{\mathbf{q},B}^{\parallel}(\omega) = \omega \hat{\rho}_{\mathbf{q},B}(\omega)$ holds, where $\hat{\rho}_{\mathbf{q}}(\omega)$ is the Fourier transform of the corresponding charge density operator $\hat{\rho}(x)$.

The general form of the interaction (3) includes the Coulomb interaction via the longitudinal component of the currents, and the coupling of the transverse component of the currents with the radiation field. We do not investigate the radiation interaction connected with the transverse component. The radiative field of the plasma determines the natural broadening which has already been extensively discussed in [38, 39] by using the quantum master equation approach. However we focus on the Coulomb interaction of the hydrogen atom with its surrounding charged particles in this work. In this case, the distribution and the motion of the charge carriers in the plasma produce a scalar potential which is given in terms of the longitudinal current [37]:

$$\hat{U}_{\mathbf{q},B}(\omega) = \sum_c \frac{\hat{\rho}_{\mathbf{q},B}^c(\omega)}{\epsilon_0 \mathbf{q}^2} = \sum_c \frac{\hat{j}_{\mathbf{q},B}^{\parallel,c}(\omega)}{\epsilon_0 \omega q}. \quad (6)$$

This results in the pressure broadening of the spectral lines as shown in Sec. II C 2.

The state of the total system is described by the statistical operator $\hat{\rho}(t)$. We assume that the observables \hat{A} of the subsystem A commute with the observables \hat{B} of the bath B. If only the properties of the subsystem A are relevant, we can consider the corresponding statistical operator

$$\hat{\rho}_A(t) \equiv \text{Tr}_B \hat{\rho}(t) \quad (7)$$

performing the trace over all bath variables. Then, the average value of any observable \hat{A} of the subsystem A is calculated as $\langle \hat{A} \rangle^t \equiv \text{Tr} \{ \hat{A} \hat{\rho}(t) \} = \text{Tr}_A \{ \hat{A} \hat{\rho}_A(t) \}$.

The equation of motion for the total statistical operator $\hat{\rho}(t)$ [39] reads

$$\frac{\partial}{\partial t} \hat{\rho}(t) - \frac{1}{i\hbar} [\hat{H}, \hat{\rho}(t)] = -\varepsilon [\hat{\rho}(t) - \hat{\rho}_{\text{rel}}(t)] \quad (8)$$

with the relevant statistical operator $\hat{\rho}_{\text{rel}}(t) = \hat{\rho}_A(t) \hat{\rho}_B$ which implies that the quantum systems A and B are uncorrelated. The equilibrium state $\hat{\rho}_B$ of the bath B is assumed as the grand canonical distribution

$$\hat{\rho}_B = \frac{1}{Z_B} \exp \left[-\frac{\hat{H}_B - \sum_c \mu_c \hat{N}_c}{k_B T} \right], \quad Z_B = \text{Tr}_B \exp \left[-\frac{\hat{H}_B - \sum_c \mu_c \hat{N}_c}{k_B T} \right] \quad (9)$$

with the chemical potentials μ_c of the species c . The limit $\varepsilon \rightarrow 0^+$ has to be performed after the thermodynamic limit.

A closed equation of motion can be derived for the reduced statistical operator $\hat{\rho}_A(t)$ of the subsystem A by performing the average with respect to the bath in (8). If the bath is assumed to have short memory in the sense that the correlation in the bath decays very quickly in comparison to the time evolution of the reduced system (Markov approximation), and the dynamics of the reduced system is considered only in second order with respect to \hat{H}_{int} (Born approximation), we obtain [39]

$$\frac{\partial}{\partial t} \hat{\rho}_A(t) - \frac{1}{i\hbar} [\hat{H}_A, \hat{\rho}_A(t)] = \mathcal{D}[\hat{\rho}_A(t)] \quad (10)$$

with the influence term

$$\mathcal{D}[\hat{\rho}_A(t)] = -\frac{1}{\hbar^2} \int_{-\infty}^0 d\tau e^{\varepsilon\tau} \text{Tr}_B \left[\hat{H}_{\text{int}}, \left[\hat{H}_{\text{int}}(\tau), \hat{\rho}_A(t) \hat{\rho}_B \right] \right]. \quad (11)$$

This is the quantum master equation (QME) in Born-Markov approximation. To go beyond the Born approximation, a more general solution has been given in [41].

Born approximation indicates that higher orders of the interaction Hamiltonian in the time evolution of the operator (4) can be dropped. Consequently, the time dependence in Born approximation is given by the interaction picture

$$\hat{O}^I(t, t_0) = e^{i(\hat{H}_A + \hat{H}_B)(t-t_0)/\hbar} \hat{O} e^{-i(\hat{H}_A + \hat{H}_B)(t-t_0)/\hbar}. \quad (12)$$

At $t = t_0$, the interaction picture coincides with the Schrödinger picture. Note that the time of reference t_0 is often taken as zero. In interaction picture, the QME in Born-Markov approximation reads

$$\frac{\partial}{\partial t} \hat{\rho}_A^I(t, t_0) = \mathcal{D}^I(t, t_0), \quad (13)$$

i.e., only the perturbation determines the time evolution of $\hat{\rho}_A^I(t, t_0)$ (note that \hat{H}_B commutes with $\hat{\rho}_A(t)$). The influence term in interaction representation follows as

$$\mathcal{D}^I(t, t_0) = -\frac{1}{\hbar^2} \int_{-\infty}^0 d\tau e^{\varepsilon\tau} \text{Tr}_B \left[\hat{H}_{\text{int}}^I(t, t_0), \left[\hat{H}_{\text{int}}^I(t + \tau, t_0), \hat{\rho}_A^I(t, t_0) \hat{\rho}_B \right] \right]. \quad (14)$$

In zeroth order with respect to the perturbation, $\hat{\rho}_A^I(t, t_0)$ is constant, no changing with time t .

B. The Influence Term for a Charged Particle System

In this section the master equation for the reduced statistical operator (13) shall be applied to atomic bound states in a many-particle plasma environment. However, most of the discussion is valid for a much more general case.

For the plasma, surrounding the radiating atom, the Hamiltonian is described by

$$\hat{H}_{\text{Coul}} = \sum_{c,p} \frac{\hbar^2 p^2}{2m_c} \hat{c}_p^\dagger \hat{c}_p + \frac{1}{2} \sum_{c,d,p_1 p_2, p'_1 p'_2} \frac{e_c e_d}{\epsilon_0 \Omega_0 |\mathbf{p}'_1 - \mathbf{p}_1|^2} \delta_{\mathbf{p}_1 + \mathbf{p}_2, \mathbf{p}'_1 + \mathbf{p}'_2} \delta_{\sigma_1, \sigma'_1} \delta_{\sigma_2, \sigma'_2} \hat{c}_{p_1}^\dagger \hat{d}_{p_2}^\dagger \hat{d}_{p'_2} \hat{c}_{p'_1} \quad (15)$$

where we used second quantization $\hat{c}_p, \hat{c}_p^\dagger$ for free particle states $|p\rangle = |\mathbf{p}, \sigma\rangle$ (wave vector and spin) of charge c . The grand canonical equilibrium (9) contains also the particle number operator $\hat{N}_c = \sum_p \hat{c}_p^\dagger \hat{c}_p$. The macroscopic state of the bath is fixed by the Lagrange multipliers μ_c and T . Ω_0 is the volume of the total system. Because of charge neutrality $\sum_c e_c \hat{N}_c \equiv 0$ both μ_e, μ_i are related. The photonic field $\hat{H}_{\text{photon}}^\perp$ is not relevant in our present consideration which is focussed on the Coulomb interaction with the charged particles of the bath.

The longitudinal part of the interaction Hamiltonian can be extracted from the general form \hat{H}_{int} (3) by using the expression (6) and performing the Fourier transform with respect to the time for the atomic charge density operator

$$\hat{\varrho}_{\mathbf{q},A}^I(t, t_0) = \int_{-\infty}^{\infty} \frac{d\omega}{2\pi} e^{-i\omega(t-t_0)} \hat{\varrho}_{\mathbf{q},A}^I(\omega) \quad (16)$$

so that

$$\hat{H}_{\text{int}}^{I,\parallel}(t, t_0) = \sum_{\mathbf{q}} \frac{1}{\epsilon_0 q^2 \Omega_0} \int \frac{d\omega}{2\pi} e^{-i\omega(t-t_0)} \hat{\varrho}_{\mathbf{q},A}^I(\omega) \hat{\varrho}_{-\mathbf{q},B}^I(t, t_0) \quad (17)$$

with $\hat{\varrho}_{\mathbf{q},B} = \sum_c \hat{\varrho}_{\mathbf{q},B}^c$ and $\hat{\varrho}_{\mathbf{q},B}^c = \sum_p e_c \hat{c}_{\mathbf{p}-\mathbf{q}/2, \sigma}^\dagger \hat{c}_{\mathbf{p}+\mathbf{q}/2, \sigma}$. In this work only the contribution of the electrons in the plasma is considered. The ionic contribution should be treated in another way, see Sec. IV. Coming back to the influence term (14), the factorization of the interaction Hamiltonian allows us to perform the average over the bath degrees of freedom separately

$$\begin{aligned} \mathcal{D}^I(t, t_0) = & -\frac{1}{\hbar^2} \int_{-\infty}^0 d\tau e^{\varepsilon\tau} \sum_{q,q'} \frac{1}{\epsilon_0^2 q^2 q'^2 \Omega_0^2} \int \frac{d\omega}{2\pi} \int \frac{d\omega'}{2\pi} e^{-i(\omega+\omega')(t-t_0)-i\omega'\tau} \\ & \times \left\{ \left[\hat{\varrho}_{\mathbf{q},A}^I(\omega) \hat{\varrho}_{\mathbf{q}',A}^I(\omega') \hat{\rho}_A^I(t, t_0) - \hat{\varrho}_{\mathbf{q}',A}^I(\omega') \hat{\rho}_A^I(t, t_0) \hat{\varrho}_{\mathbf{q},A}^I(\omega) \right] \langle \hat{\varrho}_{-\mathbf{q},B}^I(t, t_0) \hat{\varrho}_{-\mathbf{q}',B}^I(t + \tau, t_0) \rangle_B \right. \\ & \left. - \left[\hat{\varrho}_{\mathbf{q},A}^I(\omega) \hat{\rho}_A^I(t, t_0) \hat{\varrho}_{\mathbf{q}',A}^I(\omega') - \hat{\rho}_A^I(t, t_0) \hat{\varrho}_{\mathbf{q}',A}^I(\omega') \hat{\varrho}_{\mathbf{q},A}^I(\omega) \right] \langle \hat{\varrho}_{-\mathbf{q}',B}^I(t + \tau, t_0) \hat{\varrho}_{-\mathbf{q},B}^I(t, t_0) \rangle_B \right\} \quad (18) \end{aligned}$$

with $\langle \dots \rangle_B = \text{Tr}_B \{ \dots \hat{\rho}_B \}$. The charge density autocorrelation function $\langle \hat{\rho}_{-\mathbf{q},B}^I(t, t_0) \hat{\rho}_{-\mathbf{q}',B}^I(t + \tau, t_0) \rangle_B$ is calculated in thermodynamic equilibrium. Because of homogeneity in space and time it is $\propto \delta_{\mathbf{q}', -\mathbf{q}}$ and not depending on the time t as well as t_0 . We introduce the Laplace transform of the bath auto-correlation functions which can be also defined as the response function

$$\Gamma_r(\mathbf{q}, \omega) = \frac{1}{\hbar^2} \int_{-\infty}^0 d\tau e^{\varepsilon\tau} e^{-i\omega\tau} \langle \hat{\rho}_{-\mathbf{q},B}^I(t_0, t_0) \hat{\rho}_{\mathbf{q},B}^I(t_0 + \tau, t_0) \rangle_B. \quad (19)$$

The response function $\Gamma_r(\mathbf{q}, \omega)$ is a complex physical quantity which is related to the dynamical structure factor of the plasma or the dielectric function, as shown in the App. A. It can be decomposed into real and imaginary parts,

$$\Gamma_r(\mathbf{q}, \omega) = \frac{1}{2} \gamma_r(\mathbf{q}, \omega) + i S_r(\mathbf{q}, \omega), \quad (20)$$

where $\gamma_r(\mathbf{q}, \omega)$ and $S_r(\mathbf{q}, \omega)$ are both real functions. They fulfill the Kramers-Kronig relation and are related to the damping and the spectral line shift, respectively (see Eqs. (B9) and (B10) in App. B).

With the response function (19), we find that the influence term (14) can be rewritten as

$$\mathcal{D}^I(t, t_0) = - \sum_q \frac{1}{\epsilon_0^2 q^4 \Omega_0^2} \int \frac{d\omega}{2\pi} \int \frac{d\omega'}{2\pi} e^{i(\omega' - \omega)(t - t_0)} \Gamma_r(\mathbf{q}, -\omega') [\hat{\rho}_{\mathbf{q},A}^I(\omega), \hat{\rho}_{-\mathbf{q},A}^I(-\omega') \hat{\rho}_A^I(t, t_0)] + \text{h.c.} \quad (21)$$

The second contribution of the r.h.s. of Eq. (21) is the hermitean conjugate of the first contribution so that $\mathcal{D}^I(t, t_0)$ is a real quantity. Approximations for the response function $\Gamma_r(\mathbf{q}, \omega)$ are obtained from the approximations for the dielectric function such as the random-phase approximation and improvements accounting for collisions.

C. Atomic Quantum Master Equation

In a next step we introduce the orthonormal basis of the hydrogen bound states in the Hilbert space of the atomic subsystem to obtain the Pauli equation for population numbers and the spectral line profiles.

1. Pauli Equation for Occupation Numbers

We use the basis of hydrogen-like states $|\psi_n\rangle$ of the Hamiltonian \hat{H}_A . For the charge density operator

$$\hat{\rho}_{\mathbf{q},A} = \int d^3\bar{\mathbf{r}} e^{i\mathbf{q}\cdot\bar{\mathbf{r}}} \hat{\rho}_A(\bar{\mathbf{r}}) = \int d^3\bar{\mathbf{r}} e^{i\mathbf{q}\cdot\bar{\mathbf{r}}} [e_e \delta(\hat{\mathbf{r}}_e - \bar{\mathbf{r}}) + e_i \delta(\hat{\mathbf{r}}_i - \bar{\mathbf{r}})] = e_e e^{i\mathbf{q}\cdot\hat{\mathbf{r}}_e} + e_i e^{i\mathbf{q}\cdot\hat{\mathbf{r}}_i}, \quad (22)$$

the time dependence in the interaction picture can be written in matrix representation as ($e_e = -e_i$)

$$\hat{\rho}_{\mathbf{q},A}^I(t, t_0) = e^{\frac{i}{\hbar} \hat{H}_A(t-t_0)} \hat{\rho}_{\mathbf{q},A} e^{-\frac{i}{\hbar} \hat{H}_A(t-t_0)} = \sum_{nn'} e_e \hat{T}_{n'n} F_{n'n}(\mathbf{q}) e^{-i\omega_{nn'}(t-t_0)} \quad (23)$$

with

$$\hat{T}_{n'n} = |\psi_{n'}\rangle \langle \psi_n|, \quad (24)$$

$$\omega_{nn'} = \frac{E_n - E_{n'}}{\hbar}, \quad (25)$$

$$F_{n'n}(\mathbf{q}) = \int d^3\mathbf{r} \psi_{n'}^*(\mathbf{r}) \psi_n(\mathbf{r}) (1 - e^{-i\mathbf{q}\cdot\mathbf{r}}), \quad (26)$$

in adiabatic approximation $m_e \ll m_i$. Furthermore, the atom is assumed to be localized at $\mathbf{R} = 0$. Performing the Fourier transformation with respect to t we obtain the atomic charge density in Fourier-space

$$\hat{\rho}_{\mathbf{q},A}^I(\omega) = \sum_{nn'} e_e \hat{T}_{n'n} F_{n'n}(\mathbf{q}) 2\pi \delta(\omega - \omega_{nn'}). \quad (27)$$

With Eq. (27) the influence function (21) can be represented as

$$\mathcal{D}^I(t, t_0) = - \sum_{nn', mm', \mathbf{q}} e^{-i(\omega_{nn'} + \omega_{mm'})(t-t_0)} K_{mm'; n'n}(\mathbf{q}, \omega_{mm'}) \left\{ \hat{T}_{n'n} \hat{T}_{m'm} \hat{\rho}_A^I(t, t_0) - \hat{T}_{m'm} \hat{\rho}_A^I(t, t_0) \hat{T}_{n'n} \right\} + \text{h.c.} \quad (28)$$

with

$$K_{mm';n'n}(\mathbf{q}, \omega) = \frac{e_e^2}{\epsilon_0^2 q^4 \Omega_0^2} F_{mm'}^*(\mathbf{q}) F_{n'n}(\mathbf{q}) \Gamma_r(\mathbf{q}, \omega) \quad (29)$$

containing informations about the atomic system, the plasma bath and the interaction between them. In matrix representation the atomic QME (13) can be represented as ($|\psi_i\rangle$ - initial state, $|\psi_f\rangle$ - final state)

$$\frac{\partial}{\partial t} \rho_{A,if}^I(t, t_0) = \langle \psi_i | \mathcal{D}^I(t, t_0) | \psi_f \rangle \quad (30)$$

with the influence function

$$\begin{aligned} \langle \psi_i | \mathcal{D}^I(t, t_0) | \psi_f \rangle &= - \sum_{mn, \mathbf{q}} \left\{ e^{i\omega_{im}(t-t_0)} K_{mn;in}(\mathbf{q}, \omega_{mn}) \rho_{A,mf}^I(t, t_0) + e^{i\omega_{mf}(t-t_0)} K_{mn;nf}^*(\mathbf{q}, \omega_{nf}) \rho_{A,im}^I(t, t_0) \right. \\ &\quad \left. - e^{i(\omega_{im} + \omega_{nf})(t-t_0)} [K_{mi;fn}(\mathbf{q}, \omega_{mi}) + K_{nf;mi}^*(\mathbf{q}, \omega_{nf})] \rho_{A,mn}^I(t, t_0) \right\} \end{aligned} \quad (31)$$

with the density matrix $\rho_{A,mn}^I(t, t_0) = \langle \psi_m | \hat{\rho}_A^I(t, t_0) | \psi_n \rangle$. The corresponding atomic QME in Schrödinger picture is obtained with $\rho_{A,mn}^I(t, t_0) = e^{i\omega_{mn}(t-t_0)} \rho_{A,mn}(t)$, see Appendix B.

We investigate the diagonal elements of the density matrix by setting $i = f$ in the above expression (30). This leads to an equation for the population number $P_i(t) = \rho_{A,ii}^I(t, t_0) = \rho_{A,ii}(t)$

$$\begin{aligned} \frac{\partial P_i(t)}{\partial t} &= \sum_{n, \mathbf{q}} \left[k_{ni}(\mathbf{q}, \omega_{ni}) P_n(t) - k_{in}(\mathbf{q}, \omega_{in}) P_i(t) \right] - \sum_{n, m \neq i, \mathbf{k}} 2\text{Re} \left[e^{i\omega_{im}(t-t_0)} K_{mn;in}(\mathbf{q}, \omega_{mn}) \right] \rho_{A,mi}^I(t, t_0) \\ &\quad + \sum_{m > n, \mathbf{q}} 2\text{Re} \left\{ e^{i\omega_{nm}(t-t_0)} \left[K_{ni;mi}^*(\mathbf{q}, \omega_{ni}) + K_{mi;in}(\mathbf{q}, \omega_{mi}) \right] \right\} \rho_{A,mn}^I(t, t_0) \end{aligned} \quad (32)$$

with $k_{ab}(\mathbf{q}, \omega_{ab}) = 2 \text{Re} K_{ab;ab}(\mathbf{q}, \omega_{ab}) = e_e^2 |F_{ab}(\mathbf{q})|^2 \gamma_r(\mathbf{q}, \omega_{ab}) / (\epsilon_0^2 q^4 \Omega_0^2)$, where expression (20) is used and the indices m and n are interchanged in the derivation. The interaction picture shows a slow time dependence in $\rho_{A,nm}^I(t, t_0)$ owing to the influence of the bath, Eq. (13), and a quick time variation due to the factor $e^{i\omega_{nm}(t-t_0)}$ with $\omega_{nm} \neq 0$. The second and third term oscillate with the characteristic transition frequencies ω_{nm} and ω_{im} , respectively. Subsequently their contributions vanish when averaging over relative larger time interval in comparison with the inverse of the characteristic transition frequencies, because the population numbers are approximately constant. This is the so-called *Rotating Wave Approximation* (RWA). For the long-term evolution of the reduced system the nondiagonal elements in Eq. (32) can be neglected and consequently we obtain a closed rate equation for the population number – the Pauli equation:

$$\frac{\partial P_i(t)}{\partial t} = \sum_{n, \mathbf{q}} \left[k_{ni}(\mathbf{q}, \omega_{ni}) P_n(t) - k_{in}(\mathbf{q}, \omega_{in}) P_i(t) \right]. \quad (33)$$

Comparing with the standard form of the Pauli equation $\frac{\partial}{\partial t} P_i(t) = \sum_n [w_{n \rightarrow i} P_n(t) - w_{i \rightarrow n} P_i(t)]$, we have for the transition rates

$$w_{n \rightarrow i} = \sum_{\mathbf{q}} k_{ni}(\mathbf{q}, \omega_{ni}) = \sum_{\mathbf{q}} \frac{e_e^2 |F_{ni}(\mathbf{q})|^2 \gamma_r(\mathbf{q}, \omega_{ni})}{\epsilon_0^2 q^4 \Omega_0^2}, \quad w_{i \rightarrow n} = \sum_{\mathbf{q}} k_{in}(\mathbf{q}, \omega_{in}) = \sum_{\mathbf{q}} \frac{e_e^2 |F_{in}(\mathbf{q})|^2 \gamma_r(\mathbf{q}, \omega_{in})}{\epsilon_0^2 q^4 \Omega_0^2}. \quad (34)$$

To derive the Pauli equation we used the RWA which neglects quickly oscillating terms. Also the dependence on the time t_0 where the interaction picture coincides with the Schrödinger picture disappears. The validity of the RWA in the theory of open quantum systems is under discussion. The dynamics is modified if contributions of the right hand side of Eq. (32) are dropped. In our investigation we found that if the RWA is carried out prematurely, it will be inappropriate to describe the dissipative properties of the relevant atomic system (Rydberg states) and result in erroneous transition rates. More details on that can be found in Appendix B. The nondiagonal elements of Eq. (30) are also discussed there.

2. Quantum Kinetic Approach to Spectral Line Profile

In open quantum system theory one separates a reduced subsystem out from the total quantum system, which includes all relevant observables that one is interested in. The remaining degrees of freedom are treated as irrelevant

for the dynamical behavior and are denoted as the observables of the bath. However, the selection of the relevant observables that are appropriate to describe the dynamics of the system depends sensitively on the physical problems that we tackle.

For instance, the degrees of freedom of the emitted photons are irrelevant for the dynamics of the population numbers of the atomic energy eigenstates and therefore can be considered as part of the bath in the derivation of the Pauli equation. This consideration is also applied in the derivation of the natural line width of the spectral line profile [38, 39]. In contrast, these degrees of freedom are most important for the description of the spectral line profile in a plasma environment where we obtain the spectral line shapes by measuring the energy of the emitted photons. The emitted photons are therefore relevant degrees of freedom. To correctly describe the spectral line shapes via the open quantum system theory, we must extend the reduced system by including the set of the degrees of freedom of the emitted photons. This means that the radiation field together with the atomic system should be considered as the reduced system to be described by the QME, and the surrounding plasma is the bath coupled to the system by Coulomb interaction.

Absorption as well as spontaneous and induced emission coefficients, related by the Einstein relation, are obtained from QED where the transverse part of the Maxwell field

$$\hat{H}_{\text{photon}}^{\perp} = \sum_{\mathbf{k}, s} \hbar \omega_{\mathbf{k}, s} \hat{n}_{\mathbf{k}, s} \quad (35)$$

is quantized and denoted by the photon modes $|\mathbf{k}, s\rangle$. The frequency $\omega_{\mathbf{k}} = c|\mathbf{k}| = 2\pi c/\lambda$ is the dispersion relation for the frequency as a function of the wave number λ . $\hat{n}_{\mathbf{k}, s} = \hat{b}_{\mathbf{k}, s}^{\dagger} \hat{b}_{\mathbf{k}, s}$ is the occupation number with the polarization $s = 1, 2$. As mentioned above, the photon field must be treated as part of the reduced system with the Hamiltonian $\hat{H}_S = \hat{H}_A + \hat{H}_{\text{photon}}^{\perp}$, and the eigenstates will be denoted by the expression $|\tilde{n}\rangle = |\psi_n, N_n(\mathbf{k}, s)\rangle$ containing corresponding quantum numbers for the eigenenergy $\tilde{E}_n = E_n + \sum_{\mathbf{k}, s} N_n(\mathbf{k}, s) \hbar \omega_{\mathbf{k}, s}$ with the occupation number $N_n(\mathbf{k}, s)$ of the mode $|\mathbf{k}, s\rangle$.

Emission and absorption are described by the interaction Hamiltonian, see Eq. (3), $\hat{H}^{\text{rad}} = \int d^3\mathbf{r} \hat{\mathbf{j}}_A^{\perp} \cdot \hat{\mathbf{A}}_{\text{ph}} = \int d^3\mathbf{r} \hat{\mathbf{d}}_A \cdot \hat{\mathbf{E}}_{\text{ph}}$ after integration by parts with the atomic dipole operator $\hat{\mathbf{d}}_A$. The decomposition of the electric field of the photon subsystem (two polarization vectors $\hat{\mathbf{e}}_{\mathbf{k}, s}$) is

$$\hat{\mathbf{E}}_{\text{ph}} = i \sum_{\mathbf{k}, s} \sqrt{\frac{\hbar \omega_{\mathbf{k}}}{2\Omega_0}} \hat{\mathbf{e}}_{\mathbf{k}, s} [\hat{b}_{\mathbf{k}, s} - \hat{b}_{\mathbf{k}, s}^{\dagger}]. \quad (36)$$

For a given measured photon mode $|\bar{\mathbf{k}}, \bar{s}\rangle$ in the experiment, only the mode with $\mathbf{k} = \bar{\mathbf{k}}$ and $s = \bar{s}$ in the Hamiltonian \hat{H}^{rad} contributes. This allows us to introduce a new operator describing emission and absorption

$$\hat{\mathbf{d}}_S = \hat{\mathbf{d}}_A \otimes (\hat{b}_{\bar{\mathbf{k}}} - \hat{b}_{\bar{\mathbf{k}}}^{\dagger}), \quad (37)$$

where the polarization index is suppressed. The initial and final states in this case are given by $|\tilde{i}\rangle = |\psi_i, N_i(\mathbf{k})\rangle$ and $|\tilde{f}\rangle = |\psi_f, N_f(\mathbf{k})\rangle$ with $N_f(\mathbf{k}) = N_i(\mathbf{k}) + \delta_{\mathbf{k}, \bar{\mathbf{k}}}$, respectively. This means that for the measured photon mode $\bar{\mathbf{k}}$ the occupation number fulfills $N_f(\bar{\mathbf{k}}) = N_i(\bar{\mathbf{k}}) + 1$, while for all other photon modes their occupation numbers remain unchanged. A shift of the eigenenergy levels is caused by the interaction with the plasma environment via the momentum exchange. Subsequently, this leads to a deviation of the measured transition frequency $\omega_{\bar{\mathbf{k}}}$ from the characteristic transition frequencies $\omega_{nn'}$ between the unperturbed atomic eigenstates $|\psi_n\rangle$. We define the deviation by using the eigenenergies \tilde{E}_n via

$$\Delta\omega_{nn'} = (\tilde{E}_n - \tilde{E}_{n'})/\hbar. \quad (38)$$

We use the interaction picture with $\hat{H}_0 = \hat{H}_S + \hat{H}_B$ so that the power spectrum $P(\omega_{\bar{\mathbf{k}}}) = \int_0^{\infty} e^{-\epsilon t} e^{\pm i\omega_{\bar{\mathbf{k}}} t} \langle \hat{\mathbf{d}}_A \rangle^t dt$ as shown in [40] in the framework of the linear-response theory can be rewritten as

$$P(\omega_{\bar{\mathbf{k}}}) = \int_0^{\infty} e^{-\epsilon t} \langle \hat{\mathbf{d}}_S \rangle^t dt = \sum_{if} \mathcal{L}_{i,f}, \quad (39)$$

where the photon frequency is absorbed by the new dipole operator $\hat{\mathbf{d}}_S$ of the reduced system (including photons) and

$$\langle \hat{\mathbf{d}}_S \rangle^t = \text{Tr}\{\hat{\rho}_S(t) \hat{\mathbf{d}}_S\} = \sum_{if} \rho_{S,fi}^I(t) \mathbf{d}_{S,if}^I(t) \quad (40)$$

with $\rho_{S,fi}^I(t)$ being the solution of the QME in interaction picture (see Eq. (44)), and the matrix elements $\mathbf{d}_{S,if}^I(t) = \langle \psi_i | \mathbf{d}_A | \psi_f \rangle e^{-i\Delta\omega_{if}t}$. Consequently, the spectral line shape $\mathcal{L}_{i,f}$ in Eq. (44) can be written as

$$\mathcal{L}_{i,f} = \int_0^\infty dt e^{-\epsilon t} \rho_{S,fi}^I(t) \mathbf{d}_{S,if}^I(t). \quad (41)$$

In order to obtain the solution of the QME, a similar reduced charge density operator containing the photon information as in Eq. (37) can be introduced for the extended reduced system

$$\hat{\rho}_{\mathbf{q},S} = \hat{\rho}_{\mathbf{q},A} \otimes (\hat{b}_{\bar{\mathbf{k}}} - \hat{b}_{\bar{\mathbf{k}}}^\dagger). \quad (42)$$

Using the basis set $|\tilde{n}\rangle$ of the unperturbed reduced system, we obtain the matrix elements of the reduced charge density operator $\hat{\rho}_{\mathbf{q},S}^I(t)$ at time t

$$\langle \tilde{n}' | \hat{\rho}_{\mathbf{q},S}^I(t) | \tilde{n} \rangle = e_e F_{n'n}(\mathbf{q}) e^{i\Delta\omega_{n'n}t} \left[\delta_{N_{n'}(\bar{\mathbf{k}}), N_n(\bar{\mathbf{k}})-1} - \delta_{N_{n'}(\bar{\mathbf{k}}), N_n(\bar{\mathbf{k}})+1} \right],$$

where the Kronecker's delta is connected to the atomic emission and absorption with the transition frequency $\omega_{n'n}$. Performing the Fourier transform with respect to the time t , we obtain the reduced charge density operator in Fourier-space

$$\hat{\rho}_{\mathbf{q},S}(\omega) = \sum_{n'>n} e_e \hat{T}_{n'n}^- \cdot F_{n'n}(\mathbf{q}) \delta(\omega - \Delta\omega_{n'n}) - \sum_{n'<n} e_e \hat{T}_{n'n}^+ \cdot F_{n'n}(\mathbf{q}) \delta(\omega + \Delta\omega_{nn'}) \quad (43)$$

with $\hat{T}_{n'n}^- = |\tilde{n}'\rangle\langle\tilde{n}| \cdot \delta_{N_{n'}(\bar{\mathbf{k}}), N_n(\bar{\mathbf{k}})-1}$ denoting the one photon absorption and $\hat{T}_{n'n}^+ = |\tilde{n}'\rangle\langle\tilde{n}| \cdot \delta_{N_{n'}(\bar{\mathbf{k}}), N_n(\bar{\mathbf{k}})+1}$ - the one photon emission.

The QME in RWA in interaction picture can be written in terms of the matrix element $\rho_{S,fi}^I(t) = \langle \tilde{f} | \hat{\rho}_S^I(t) | \tilde{i} \rangle$:

$$\frac{\partial \rho_{S,fi}^I(t)}{\partial t} = -\Gamma_{fi}^{BS}(\omega_{\bar{\mathbf{k}}}) \rho_{S,fi}^I(t) + \Gamma_{fi}^V \rho_{S,fi}^I(t), \quad (44)$$

which is shown in detail in Appendix C. The influence function, the right side of the Eq. (44), characterizes the spectral intensity of the emitted photons by a coefficient $\Gamma_{fi}^{BS}(\omega_{\bar{\mathbf{k}}})$ describing the shift of the eigenenergy levels and the pressure broadening

$$\Gamma_{fi}^{BS}(\omega_{\bar{\mathbf{k}}}) = \sum_{n,\mathbf{q}} \{ K_{nf;fn}(\mathbf{q}, \Delta\omega_{nf}) + K_{nf;fn}(\mathbf{q}, -\Delta\omega_{fn}) + K_{ni;in}^*(\mathbf{q}, \Delta\omega_{ni}) + K_{ni;in}^*(\mathbf{q}, -\Delta\omega_{in}) \} \quad (45)$$

and a coefficient Γ_{fi}^V describing the vertex correction

$$\Gamma_{fi}^V = \sum_{\mathbf{q}} \{ K_{ii;ff}(\mathbf{q}, \Delta\omega_{ff}) + K_{ii;ff}(\mathbf{q}, -\Delta\omega_{ff}) + K_{ff;ii}^*(\mathbf{q}, \Delta\omega_{ii}) + K_{ff;ii}^*(\mathbf{q}, -\Delta\omega_{ii}) \}, \quad (46)$$

The vertex correction has no dependence on the photon frequency $\omega_{\bar{\mathbf{k}}}$ and contributes only beyond the dipol approximation. Formally integrating the expression (44) yields

$$\rho_{S,fi}^I(t) = \rho_{S,fi}^I(0) \cdot e^{-\{\Gamma_{fi}^{BS}(\omega_{\bar{\mathbf{k}}}) - \Gamma_{fi}^V\}t}. \quad (47)$$

Inserting this formal solution into the Eq. (41), the line shape function can be expressed as

$$\mathcal{L}(\omega_{\bar{\mathbf{k}}})_{i,f} \propto \frac{1}{\omega_{\bar{\mathbf{k}}} - \omega_{if} + i\epsilon - i\Gamma_{if}^{BS}(\omega_{\bar{\mathbf{k}}}) + i\Gamma_{if}^V}. \quad (48)$$

The expression (48) coincides with the result of the unified theory for spectral line profiles [42] if only the electron contribution (impact approximation) is considered. Note that the unified theory gives the result in Born approximation with respect to the interaction with the surrounding plasma, what corresponds to the Born-Markov approximation for the coupling to the plasma considered as the bath. Strong coupling of the radiator to the perturbing environment has been treated in the Green function approach using a T-matrix approximation, see [42]. The improvement of the Born-Markov approximation for the QME considering strong interactions and the ionic contribution of the plasma environment, given by the microfield distribution, will be discussed below in Sec. IV.

III. ROBUST CIRCULAR WAVE PACKET AND TRANSITION RATES

An advantage of the QME is the possibility to introduce optimal (robust) states which allows the transition from a quantum description to a classical one. In the case of Rydberg atoms, one considers electrons in highly excited hydrogen states. With increasing quantum number \bar{n} , a pure hydrogen orbital can be formed only if the atom is well isolated from external influences. When the interaction with the bath is comparable or greater than the differences of atomic energy eigenstates E_n for \bar{n} near a fixed value n_0 , the wave packet description is more appropriate to describe the evolution of the system, in particular transition rates. For a local interaction such as the Coulomb potential, the position \mathbf{r} of the atomic electron enters the interaction part of the Hamiltonian, and localization is favored because \mathbf{r} commutes with \hat{H}_{int} and is a conserved quantity with respect to this part of the Hamiltonian.

In addition, the introduction of the wave packet description may allow us to investigate the boundary between the quantum and classical descriptions of systems. In fact, since the introduction of quantum mechanics many physicists attempted to establish the connections between these descriptions of nature by exhibiting the so-called coherent wave packet. One of the famous examples is the well known coherent state of the linear harmonic oscillator [43] which may be regarded as an excellent example to describe the macroscopic limit of a quantum mechanical system according to the correspondence principle. For the Coulomb problem, e.g. the hydrogen atom, many attempts to construct localized semi-classical solutions of the coherent-state type have been made [44–48]. Note that the hydrogen atom is equivalent to the four-dimensional harmonic oscillator so that coherent wave packets can be introduced accordingly [46]. Recently, Makowski and Peplowski constructed very well-localized two-dimensional wave packets for two different potentials [49, 50] where a very good quantum-classical correspondence is observed. In the present paper we use Brown's circular-orbit wave packet [44, 51] as a quasiclassical representation to describe the highly excited Rydberg states of the hydrogen atom.

A. Wave Packet for Circular Motion

Within the QME approach, the state of the relevant system $\hat{\rho}_S$ is of interest, and we can represent the statistical operator by the density matrix $\rho_{S,mn} = \langle m | \hat{\rho}_S | n \rangle$ with respect to the states $|n\rangle$ of the system. For the representation, one can use the orthonormal basis set of energy eigenstates of the unperturbed bound system according to the interaction picture. In the case considered here these are the hydrogen orbitals. For a complete orthonormal basis the scattering states must be also included. The hydrogen orbitals are long-living if the perturbation by the surrounding plasma is small. If the broadening of the energy levels remains small compared to the distance between neighbored energy eigenvalues, the transition rate due to collisions with the plasma is small.

At high excitation (Rydberg states), the interaction effects are no longer small compared to the level distance, and the pure quantum state has only a short life time. Therefore one can look for more robust states that are formed as superposition of energy eigenstates but are more stable in the time evolution. In particular, the Coulomb interaction contains the position operator, and localized states are more robust with respect to the interaction with the surrounding plasma. To find the robust states one has to optimize the quantum states. For simplicity, we restrict ourselves to circular-orbit eigenfunctions of the hydrogen atom. In this section, we use the notation n for the principal quantum number,

$$\psi_n(\mathbf{r}) = \langle \mathbf{r} | \psi_{n,n-1,n-1} \rangle = c_n \left(\frac{r}{a_B} \right)^{n-1} e^{-r/(na_B)} \sin^{n-1}(\theta) e^{i(n-1)\phi}, \quad (49)$$

where $c_n = (2/(na_B))^{3/2} [2n(2n+1)!]^{-1/2}$ denotes the normalization constant. Furthermore, in this section we use the abbreviation $\psi_n(\mathbf{r})$ for the circular wave function $\psi_{n,n-1,n-1}(\mathbf{r})$. It could be seen from Eq. (49) that the hydrogen electron in this eigenstate is already excellently localized in the radial (r) and polar (θ)-direction. To achieve the localization with respect to the azimuthal direction angle ϕ , the wave packet can be introduced.

The circular-orbit wave packet of the hydrogen atom is a coherent state constructed from the superposition of circular-orbit eigenfunctions of the hydrogen atom with a Gaussian weighting function around a large principal quantum number n_0 [51]:

$$|G_{n_0,\phi_0}\rangle = \sum_n \frac{g_{n_0,n}}{\sqrt{\mathcal{N}_{n_0}}} e^{i(n-1)\phi_0} |\psi_n\rangle \quad (50)$$

with the Gaussian factor and the normalization factor respectively

$$g_{n_0,n} = \exp \left\{ -\frac{(n-n_0)^2}{4\sigma_{n_0}^2} \right\}, \quad \mathcal{N}_{n_0} = \sum_{n=1}^{\infty} \exp \left\{ -\frac{(n-n_0)^2}{2\sigma_{n_0}^2} \right\}, \quad (51)$$

where σ_{n_0} is the standard deviation considered as fixed parameter for n_0 . Without loss of generality we can put $\phi_0 = 0$ because it fixes, as a phase factor, only the initial position of the wave packet at the azimuthal angle ϕ . We drop ϕ_0 in the following. Due to the superposition with a Gaussian factor, we have also good localization with respect to ϕ in the wave packet description (50). The actual Hilbert space $\mathcal{H}_{n,n-1,n-1}$ considered here is only a subspace of the entire Hilbert space \mathcal{H} of the hydrogen atom. The generalization to the full Hilbert space to include all bound and scattering states could be done straightforwardly.

The time-dependent wave packet in the coordinate representation in terms of spherical coordinates is given by

$$\langle \mathbf{r} | G_{n_0} \rangle^t = \sum_n \frac{g_{n_0,n}}{\sqrt{\mathcal{N}_{n_0}}} e^{iE_n t/\hbar} \psi_n(\mathbf{r}) \quad (52)$$

with $E_n = \text{Ry}/n^2$ and $\text{Ry} = 13.6 \text{ eV}$. For an appropriate Gaussian factor only the terms with principal quantum number adjacent to n_0 contribute. Therefore we can use the central quantum number n_0 to approximate other states in radial and θ -direction. In addition, for short-term time evolution the energy E_n in the factor $e^{iE_n t/\hbar}$ in Eq. (52) can be expanded around n_0 up to the second order, which relates directly to the quantum revival, see below. The probability distribution of the wave packet can be represented as

$$|\langle \mathbf{r} | G_{n_0} \rangle^t|^2 = \sum_{m,n} c_{n_0}^2 \left(\frac{r}{a_B} \right)^{2n_0-2} e^{-2r/(n_0 a_B)} \sin^{2n_0-2}(\theta) \cdot e^{-(a_1 - i\omega_{\text{rev}} t)(n-n_0)^2 - (a_1 + i\omega_{\text{rev}} t)(m-n_0)^2 + i(\phi - \omega_{\text{cl}} t)(n-m)} \quad (53)$$

with $a_1 = 1/(4\sigma_{n_0}^2)$, $\omega_{\text{cl}} = |E'_{n_0}|/\hbar = 2\text{Ry}/(\hbar n_0^3)$ and $\omega_{\text{rev}} = |E''_{n_0}|/(2\hbar) = 3\text{Ry}/(\hbar n_0^4)$, where E'_{n_0} and E''_{n_0} are the first and second derivatives of E_n with respect to the main quantum number n at n_0 , respectively. As pointed out in [52], ω_{cl} relates to the classical Kepler period $T_{\text{cl}} = 2\pi r_{\text{cl}}/v_{\text{cl}}$ for the Kepler trajectory with $r_{\text{cl}} = n_0^2 a_B$ and $v_{\text{cl}} = \sqrt{\text{Ry}/(m_e n_0^2)}$, and the quantum revival period can be defined by ω_{rev} .

For highly excited states $|x| \ll n_0$ with $x = n - n_0$ and $|y| \ll n_0$ with $y = m - n_0$, the sum $\sum_{m,n}$ can be replaced by the integral $\int_{-\infty}^{\infty} dx \int_{-\infty}^{\infty} dy$. Integrating over the variables r and θ and performing the integral over x, y yields the probability distribution of the wave packet

$$|G_{n_0}(\phi, t)|^2 \sim \sqrt{\frac{\pi^2}{a_1^2 + (\omega_{\text{rev}} t)^2}} \exp \left[-\frac{\phi_{\text{cl}}^2(t)}{2[a_1^2 + (\omega_{\text{rev}} t)^2]/a_1} \right] \quad (54)$$

with $\phi_{\text{cl}}(t) = \phi - \omega_{\text{cl}} t$. From this probability distribution the time-dependent width of the wave packet for a Rydberg electron can be extracted

$$\sigma_{n_0}^\phi(t) = \sqrt{[a_1^2 + (\omega_{\text{rev}} t)^2]/a_1} = \sqrt{\frac{1}{4\sigma_{n_0}^2} + \frac{\sigma_{n_0}^2 (E''_{n_0} t)^2}{\hbar^2}}. \quad (55)$$

For the initial time $t = 0$, we have $\sigma_{n_0}^\phi = 1/(2\sigma_{n_0})$. The expression (54) also shows that on such a short time scale the central position of the probability distribution is exactly determined by the Kepler motion. The localized wave packet for the hydrogen atom moves along the classical Keplerian trajectory of the electron and its width broadens. With time evolution the localization of the wave packet is destroyed and interference fringes of different eigenstates are displayed. On a much longer time scale $T_{\text{rev}} = 2\pi/\omega_{\text{rev}}$, the wave packet finally reverses itself, which is the above mentioned quantum revival as indicated in Eq. (54).

The dynamics of the wave packet shown above is purely due to quantum mechanical evolution without plasma surroundings. Within a plasma environment, the hydrogen atom undergoes interactions with the plasma particles which results in the shift of the eigenenergy levels, the broadening of plasma spectral lines, the screening of the Coulomb potential, the localization of the hydrogen atom (proton and bound electron), etc. In this work we concentrate on the localization of the bound electron immersed in a plasma environment.

The scattering of the bound electron by free plasma electrons results in the localization of the electron of the hydrogen atom, i.e. the collisions with the plasma tend to localize the Rydberg electron and to narrow the wave packet. As in the case of free particles in a surrounding environment [2], the spreading of the wave packet competes with the localization effect induced by the plasma environment. The optimum width of a Gaussian wave packet where both effects, localization and quantum diffidence, nearly compensate, describes a state which is nearly stable in time and is denoted as robust state.

In this work we are interested in time scales, which are even smaller than the classical Keplerian periodicity T_{cl} . We assume that on such a short time scale a Rydberg electron behaves like a free electron because of the weak coupling between the electron and the proton. Comparing with the relaxation processes, which describe the inelastic coupling

between the internal energy eigenstates and the surrounding environment, the quasiclassical Kepler motion of the wave packet is assumed to be influenced by the elastic scattering of the Rydberg electrons with its surroundings. Similarly as in the case of the quantum Brownian motion of a free particle [2], the equation of motion for the reduced density matrix with respect to variable $x = r_{\text{cl}} \phi$ obeys

$$\frac{\partial}{\partial t} \rho(x, x', t) = -\Lambda_{R_n} (x - x')^2 \quad (56)$$

with the localization rate

$$\Lambda_{R_n} = \frac{n_{\text{pl}}}{\pi(2\pi\hbar)^2} \int_0^\infty dq \frac{q^4}{3} V_{\mathbf{q}}^2 F_{nn}^2(\mathbf{q}) \sqrt{\frac{m_e}{2\pi k_B T q^2}} e^{-\hbar^2 q^2 / (8m_e k_B T)}, \quad (57)$$

describing how fast interferences of an entangled system of extension $|x - x'|$ are suppressed, for details see Appendix D. According to [2], the optimal width of the wave packet is defined by equilibrating the interplay between the spreading of the wave packet and the localization of the wave packet and reads:

$$\sigma_n^{\text{cl}} = \frac{1}{2} \left(\frac{\hbar}{m_e \Lambda_{R_n}} \right)^{1/4}. \quad (58)$$

As a consequence, an optimal width σ_{n_0} can be calculated using the relation (55) for $t = 0$ and the relation $\sigma_{n_0}^\phi = \sigma_{n_0}^{\text{cl}} / r_{\text{cl}}$ so that

$$\sigma_{n_0} = \frac{r_{\text{cl}}}{2 \sigma_{n_0}^{\text{cl}}}. \quad (59)$$

For the plasma with temperature $T = 300\text{K}$ and density $n_{\text{pl}} = 10^9 \text{cm}^{-3}$, we obtain an optimal width $\sigma_{n_0} = 0.75$ for $n_0 = 13$, which will be shown in the next section to be appropriate to describe the transition rate.

In table I we show the dependence of the localization rates on the plasma parameters for different principal quantum numbers. For given temperature and density, the localization rate decreases slightly with the increasing quantum number n_0 . At a fixed temperature, the localization rate is raised drastically when the plasma density increases. At the same time, the localization rate shows only a weak dependence on the plasma temperature.

T [K]	$n_{\text{pl}} [\text{cm}^{-3}]$	quantum number n_0			
		10	20	30	40
100	10^9	5.722	5.722	5.722	5.721
	10^{12}	180.3	180.1	180.0	179.7
	10^{15}	5090	4969	4813	4645
1000	10^9	5.722	5.722	5.722	5.722
	10^{12}	180.9	180.8	180.7	180.6
	10^{15}	5619	5549	5474	5399
10000	10^9	5.722	5.722	5.722	5.722
	10^{12}	180.9	180.9	180.9	180.9
	10^{15}	5696	5670	5645	5619

Table I: Localization rate Λ_{R_n} (57) in units $[10^{23} \text{cm}^{-2} \text{s}^{-1}]$ for different plasma densities and temperatures.

The transition between descriptions of the bound electron in hydrogen atom by the wave packet and the pure quantum eigenstate may be determined by comparing the optimal width (58) with the orbit radius $r_{n_0} = r_{\text{cl}} = n_0^2 a_{\text{B}}$. For this, a function $b(n_0, n_{\text{pl}}, T)$

$$b(n_0) = b(n_0, n_{\text{pl}}, T) = \frac{\sigma_{n_0}^{\text{cl}}}{r_{n_0}} - 1 \quad (60)$$

can be introduced. For the given electron density n_{pl} and temperature T of the plasma, quantum mechanical descriptions is valid for $b(n_0) > 0$, and for the opposite case ($b(n_0) < 0$), the wave packet descriptions can be used.

In Fig. 1 we show this function for different plasma densities at the given temperature $T = 300 \text{K}$. With the increase of the plasma density the principal quantum number n_{cr} at $b(n_{\text{cr}}) \approx 0$ characterizing the change from a pure quantum description to a classical description drops drastically.

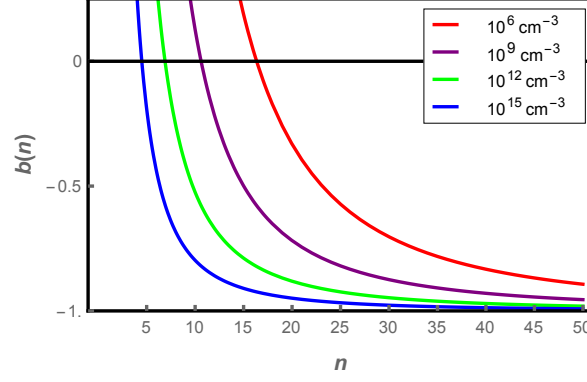


Figure 1: Boundary between classical and quantum mechanical descriptions of the hydrogen electron at $T = 300$ K for different densities.

We discussed the descriptions of the bound electron, in particular the validity of the wave packet description. We have shown that this question is related to the localization of the wave packet if an optimal width of the wave packet is assumed, which also has a dependence on the mass of the localized object as shown in Eq. (58). Similar considerations can be made for the free electrons and ions in the plasma (see. Sec. IV).

B. Transition Rates

We are interested in a matrix representation of the QME. We use robust states $|i\rangle = |G_{n_i}\rangle$ for the initial state and $|f\rangle = |G_{n_f}\rangle$ for the final state to investigate the atomic transition rates of the Rydberg states. For the reduced Hilbert space $\mathcal{H}_{n,n-1,n-1}$ used to construct the circular-orbit wave packet, there is no completeness relation $\sum_n |n\rangle\langle n| = \hat{1}$ because non-circular orbits are missing. Only if we project on the reduced Hilbert space, this relation can be applied. A more general discussion about the completeness relation in the wave packet case is found in Refs. [53, 54]. Therewith the charge density operator in Hilbert space $\mathcal{H}_{n,n-1,n-1}$ is expressed as

$$\hat{\varrho}_{\mathbf{q},A}^I(t) = \sum_{mn} e_e \hat{T}_{mn} F_{mn}(\mathbf{q}) e^{i\omega_{mn}t}. \quad (61)$$

In Fourier-space the charge density operator reads

$$\hat{\varrho}_{\mathbf{q},A}^I(\omega) = \sum_{mn} e_e \hat{T}_{mn} F_{mn}(\mathbf{q}) 2\pi\delta(\omega + \omega_{mn}). \quad (62)$$

Note that the operators given in this section are all projected on the reduced Hilbert space $\mathcal{H}_{n,n-1,n-1}$. The use of the full Hilbert space is more complex and should be worked out in future investigations.

In the present section, the diffusion of the wave packet with the center quantum number n_0 is of essential interest. The dynamics along the classical trajectory, shown in the previous section, is given by $\phi_{\text{cl}}(t)$. To investigate the diffusion of the wave packet with respect to the quantum number n , we come back to the QME in which the influence function for the wave packet in Hilbert space $\mathcal{H}_{n,n-1,n-1}$ is obtained by inserting the charge density operator (62) into equation (21)

$$\mathcal{D}^I[\hat{\rho}_A^I(t)] = - \sum_{nn',mm',\mathbf{q}} e^{-i(\omega_{nn'} + \omega_{mm'})(t-t_0)} K_{mm';n'n}(\mathbf{q}, \omega_{mm'}) \left\{ \hat{T}_{n'n} \hat{T}_{m'm} \hat{\rho}_A^I(t, t_0) - \hat{T}_{m'm} \hat{\rho}_A^I(t, t_0) \hat{T}_{n'n} \right\} + \text{h.c.} \quad (63)$$

The influence function in RWA can be represented in matrix representation as

$$\begin{aligned} \langle f | \mathcal{D}^I[\hat{\rho}_A^I(t)] | i \rangle &= \sum_{s,h,\mathbf{q}} \mathcal{G}_{n_f,s}^{n_i,h} \left\{ K_{ss;hh}(\mathbf{q}, \omega_{ss}) + K_{hh;ss}^*(\mathbf{q}, \omega_{hh}) \right. \\ &\quad \left. - \sum_n \{ K_{sn;sn}(\mathbf{q}, \omega_{sn}) + K_{hn;nh}^*(\mathbf{q}, \omega_{hn}) \} \right\} \rho_{A,sh}^I(t) \end{aligned} \quad (64)$$

with

$$\mathcal{G}_{n_f,s}^{n_i,h} = \frac{g_{n_f,s} \cdot g_{n_i,h}}{\sqrt{\mathcal{N}_{n_f} \mathcal{N}_{n_i}}}, \quad (65)$$

where the g -function is given by Eq. (51). After decomposition of the response function $\Gamma_r(\mathbf{q}, \omega) = \gamma_r(\mathbf{q}, \omega)/2 + iS_r(\mathbf{q}, \omega)$, we have the dissipator for the circular wave packet

$$\langle f | D^I [\hat{\rho}_A^I(t)] | i \rangle = -\frac{1}{2} \sum_{s,h} \mathcal{G}_{n_f,s}^{n_i,h} \left\{ D_1 + D_2 + D_3 \right\} \rho_{A,sh}^I(t) \quad (66)$$

with

$$D_1 = \sum_{\mathbf{q}} V_{\mathbf{q}}^2 |F_{ss}(\mathbf{q}) - F_{hh}(-\mathbf{q})|^2 \gamma_r(\mathbf{q}, 0), \quad (67)$$

$$D_2 = \sum_{\mathbf{q}} \{k_{hs}(\mathbf{q}, \omega_{hs}) + k_{sh}(\mathbf{q}, \omega_{sh})\}, \quad (68)$$

$$D_3 = \sum_{n \neq s,h} \sum_{\mathbf{q}} \{k_{sn}(\mathbf{q}, \omega_{sn}) + k_{hn}(\mathbf{q}, \omega_{hn})\}. \quad (69)$$

This dissipator, describing the decoherence of the nondiagonal elements of the wave packet, has three different contributions. D_1 originates from the vertex correction and contributes only beyond the dipol approximation. D_3 represents the contributions of all intermediate transitions. The transition between the contributing initial state s and final state h is hidden in D_2 and from which the transition rates for the wave packet can be defined (see also Eq (B17) in App. B and the discussion there):

$$\mathcal{W}_{n_i \rightarrow n_f} = \sum_{s,h} \mathcal{G}_{n_f,s}^{n_i,h} \cdot w_{h \rightarrow s} \quad (70)$$

with the atomic transition rate given in Eq. (34).

In collision theory, the T-matrix $\hat{T} = \hat{V} + \hat{V} \hat{G}_0 \hat{V} + \hat{V} \hat{G}_0 \hat{V} \hat{G}_0 \hat{V} + \dots$ is used to calculate the cross sections and the transition rates. Comparison with the Born approximation implemented in the derivation of the QME (13) shows that only the first term \hat{V} in T-matrix is taken into account. In order to obtain a better description of the collision effects in plasma, higher-order terms should be evaluated. We use a semiclassical approximation reported in Ref. [58] to describe the modification of the transition rate due to the collision effects in plasma, which is given by

$$f(n, \Delta n, \Theta) = \ln \left[1 + \frac{1}{\Delta n \Theta (1 + 2.5 n \Theta / \Delta n)} \right] \cdot \left[\ln \left(1 + \frac{1}{\Delta n \Theta} \right) \right]^{-1}, \quad \Theta = \sqrt{\frac{|E_n|}{k_B T}} \quad (71)$$

with $\Delta n = n - n'$ and the binding energy E_n for the hydrogen atom. Therefore the modified transition rate for the wave packet description may be written as

$$\mathcal{W}_{n_i \rightarrow n_f} = \sum_{s,h} \mathcal{G}_{n_f,s}^{n_i,h} \cdot w_{h \rightarrow s} \cdot f(h, |h - s|, \Theta). \quad (72)$$

In Fig. 2 we show the transition rates calculated from the expression (72) for two different values for the width of the hydrogenic wave packet. Comparing with the experimental data of Helium, it can be seen that the transition rates calculated with the wave packet width $\sigma_{n_0} = 0.75$, evaluated using Eq. (59) for the given plasma parameters T and n_{pl} , are in best agreement. The agreement reveals the coherent wave packet character of the Rydberg electron.

The comparison between the results of the classical Monte-Carlo simulation and the experimental data indicates that a classical treatment is more appropriate to calculate the transition rates of the highly excited states. In the classical Monte-Carlo simulation, the highly excited free electron is treated as a point in an 18 dimensional phase space which behaves in accordance with classical laws under the influence of the Coulomb interactions [55]. From the quantum mechanical point of view, this treatment is equivalent to represent the electron as an incoherent wave packet with vanishing width.

Another comparison for the transition rates with the initial principal quantum number $n_i = 40$ is shown in Fig. 3. From the figure the validity of the wave packet description can be also verified from the agreement between the results of classical Monte-Carlo simulations and the results calculated with the wave packet width $\sigma_{n_0} = 2$.

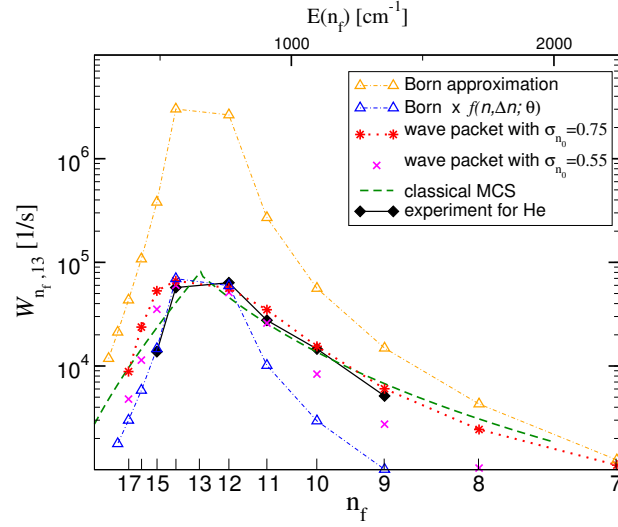


Figure 2: Transition rates of $n_i = 13$ to near n_f states induced at a $T = 300$ K electron plasma with density $n_{pl} = 10^9 \text{ cm}^{-3}$. calculated from the wave packet description with the width $\sigma_{n_0} = 0.55$ and $\sigma_{n_0} = 0.75$ compared to the results from classical Monte-Carlo simulation (MCS) [56], the calculation in Born approximation with and without collision effects from Ref. [28] and experimental data [57].

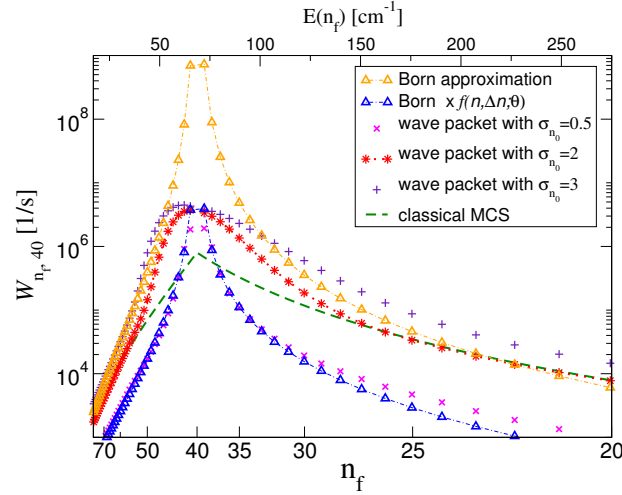


Figure 3: Transition rates of $n_i = 40$ to near n_f states induced by a $T = 20$ K electron plasma with density $n_{pl} = 10^9 \text{ cm}^{-3}$ calculated from the wave packet description with the width $\sigma_{n_0} = 0.5, 2, 3$ compared to the results from classical Monte-Carlo simulation [56] (green line) and the results in Born approximation with and without collision effects from Ref. [58].

IV. DISCUSSION AND CONCLUSION

We derived quantum master equations for an atom interacting with the charged particles of a plasma environment. In Born-Markov approximation, the influence function of the plasma environment is determined by the dynamical structure factor of the plasma. As a consequence of the atom-plasma interaction, the electrons in highly excited Rydberg states become localized. Localization of free electrons due to interactions with the environment is known from the quantum Brownian motion [2]. This may be a good approximation in the limit of highly excited Rydberg states where the mean free path of the electrons is small compared to the radius of the Kepler orbit. We derived a localization rate for electrons moving on a Kepler orbit, where the diagonal atomic formfactor appears.

Robust states are introduced as optimized wave packets. The quantum diffusion of the wave packets is nearly compensated by the localization due to collisions with the surrounding plasma. A critical quantum number n_{cr} is found. States with a lower quantum number are described by pure quantum states as solution of the atomic (hydrogen) Hamiltonian. For higher quantum numbers $n_0 > n_{cr}$, the superposition of different quantum states leads to a wave

packet characterized by an average quantum number n_0 . Consequently, classical motion (Kepler ellipses) with a corresponding Kepler radius $r_{cl} = n_0^2 a_B$ and an average azimuthal angle $\phi_{cl}(t)$ is observed. By construction, we are restricted to circular motion only. By avoiding the restriction to the Hilbert subspace of circular orbits ($l = m = n - 1$), more general Kepler orbits can be obtained taking into account all bound states for constructing the wave packet.

As another example for the use of the atomic master equation, the spectral line shape for transitions at low quantum numbers has been derived. The equivalence with a quantum statistical approach to profiles of spectral lines [42] has been shown. After decoupling the ion and electron subsystems of the plasma environment, only the electron contribution to the spectral line shape has been considered (impact approximation). The standard description of the interaction with the plasma ions is the ionic microfield. The ionic structure factor determines the microfield distribution, and a superposition of the Stark shift in the ionic microfield and the electron contribution in impact approximation leads to the line profiles as derived from the unified theory [42].

For comparison, the influence of the plasma ions on the line profile can also be calculated in Born approximation, similar to the treatment of the plasma electrons using the impact approximation. The ions localize more strongly in comparison to the electrons as a consequence of the larger localization rate (57) if the electron mass is replaced by the ion mass. In other words, for electrons in plasma under normal conditions the quantum description is applicable, whereas for ions the classical description is more appropriate. The domains within the plasma density-temperature diagram, where the robust states of the ions are localized so that the concept of the classical ionic microfield can be justified while electrons should be treated quantum mechanically, have been outlined, for instance, in Ref. [29].

In the present work, we have shown that for electrons in Rydberg states localization may occur owing to the interaction with the plasma environment. Transition rates were calculated using robust quantum states formed by wave packets. Comparing with experiments and MCS results, the use of robust quantum states gives a better agreement with measured data and classical calculations than the approach using pure hydrogen eigenenergy states. Thus, the wave packet description which accounts for localization is more appropriate not only for the ions but also for the electrons when considering highly excited Rydberg states. We performed exploratory calculations using the Brown circular-orbit wave packets. The approach can be further worked out to more general wave packets formed by the entire Hilbert space of the atomic states.

The existence of the plasma environment leads also to a reduction of the bound electron binding energy because of the screening effects in the plasma. Consequently, bound states shift into the continuum which is the so-called lowering of the continuum edge [60]. This means there is a maximum principal quantum number $n_{\max}(T, n)$ for the Rydberg states at a given plasma temperature T and a given density n where separate bound states below the continuum can be identified. The reduction of the principal quantum number n_{cr} , below which a pure hydrogen quantum state is robust, as shown in Fig. 1, has to be compared to the pressure ionization of the plasma. Using the standard expression for the lowering of the ionization potential in Ref. [62], estimations for the maximum principal quantum number n_{\max} can be made. For instance, at the plasma densities 10^9 cm^{-3} and 10^{15} cm^{-3} the maximum principal quantum numbers are $n_{\max} \approx 200$ and $n_{\max} \approx 20$, respectively. Near the continuum edge, it is difficult to distinguish between the real continuum edge and the point at which the spectroscopic series merges into a continuum due to line broadening. It would be of interest to investigate whether a wave packet description might be more suitable near the continuum edge. For this, the definition of the wave packet (50) should be extended to include the continuum states, similar to the case of free electrons where a Gaussian wave packet can be formed by plane wave states.

A fundamental issue in the theory of open quantum systems is that the subdivision of the total system into the reduced system and the bath is arbitrary and can be changed. Degrees of freedom of the bath which are strongly coupled to the reduced system may be incorporated into the reduced system, so that the bath contains only weakly coupled degrees of freedom which may be treated in Born-Markov approximation. Various approximations, in particular the Born-Markov approximation and the rotating-wave approximation, performed in the present work can be improved in future work, see also Ref. [41]. Furthermore, the electron in atom and the plasma electrons must be antisymmetrized so that exchange terms will occur. With respect to radiation processes, it is in general not the single electron which emits radiation but the whole reduced system which couples to the radiation field. As an interesting application of this aspect, the treatment of radiation from many-electron atoms, for instance the K_α radiation, is presently under investigation.

A main advantage of the QME for hydrogen Rydberg atom surrounded by a plasma is the use of robust states instead the pure hydrogen eigenenergy states. The treatment of localization allows the transition to classical physics and the very efficient use of classical descriptions, for instance in molecular-dynamical simulations. On the other side, QMEs are an essential ingredient to formulate a nonequilibrium approach for many-body systems, which can also be done on a very fundamental level as QED. The Rydberg atoms considered in the present work are an interesting object to describe the transition from the quantum microworld to macroscopic classical world where new properties such as trajectories emerge.

Acknowledgments

The authors acknowledge support within the DFG funded Special Research Unit SFB 652.

Appendix A: Dynamical Structure Factor and Response Function

The response function γ_r is the real part of the Laplace transform of the density-density correlation function. With the eigenstates $|\phi_n\rangle$ of the bath, $(\hat{H}_B - \sum_c \mu_c \hat{N}_c)|\phi_n\rangle = B_n|\phi_n\rangle$, the spectral density of the density-density correlation function follows as

$$I(\mathbf{q}, \omega) = \frac{1}{e_e^2} \sum_{n,m} \frac{e^{-\beta B_n}}{\sum_{n'} e^{-\beta B_{n'}}} \langle \phi_n | \hat{\rho}_{-\mathbf{q},B} | \phi_m \rangle \langle \phi_m | \hat{\rho}_{\mathbf{q},B} | \phi_n \rangle 2\pi \delta(\omega - B_n/\hbar + B_m/\hbar). \quad (\text{A1})$$

The spectral density is the Fourier transform of the density autocorrelation function,

$$\langle \hat{\rho}_{-\mathbf{q},B}(\tau) \hat{\rho}_{\mathbf{q},B}(0) \rangle_B = e_e^2 \int_{-\infty}^{\infty} \frac{d\omega}{2\pi} I(\mathbf{q}, \omega) e^{i\omega\tau}. \quad (\text{A2})$$

We find

$$\Gamma_r(\mathbf{q}, \omega) = \frac{e_e^2}{2\hbar^2} I(\mathbf{q}, -\omega) + i\mathcal{P} \frac{e_e^2}{\hbar^2} \int_{-\infty}^{\infty} \frac{d\omega'}{2\pi} I(\mathbf{q}, -\omega') \frac{1}{\omega - \omega'}, \quad (\text{A3})$$

where \mathcal{P} denotes the principal value of the integral.

Now we can use the fluctuation-dissipation theorem

$$\gamma_r(\mathbf{q}, \omega) = \frac{e_e^2}{\hbar^2} I(\mathbf{q}, -\omega) \quad (\text{A4})$$

and have for $S_r(\mathbf{q}, \omega)$, which determines the Lamb shift, the Kramers-Kronig relation

$$S_r(\mathbf{q}, \omega) = \mathcal{P} \frac{e_e^2}{\hbar^2} \int_{-\infty}^{\infty} \frac{d\omega'}{2\pi} I(\mathbf{q}, -\omega') \frac{1}{\omega - \omega'} = \mathcal{P} \int_{-\infty}^{\infty} \frac{d\omega'}{2\pi} 2\gamma_r(\mathbf{q}, \omega') \frac{1}{\omega - \omega'}. \quad (\text{A5})$$

The response function can be related to the dynamical structure factor (DSF) of the bath which is defined via the Fourier transform of the correlation function of the density fluctuation [59]:

$$S_B(\mathbf{q}, \omega) = \frac{1}{2\pi n_{\text{pl}} \Omega_0 e_e^2} \int_{-\infty}^{\infty} d\tau e^{i\omega\tau} \langle \delta \hat{\rho}_{\mathbf{q},B}(\tau) \delta \hat{\rho}_{-\mathbf{q},B}(0) \rangle_B, \quad (\text{A6})$$

where n_{pl} is the electron density in plasma and $\delta \hat{\rho}_{\mathbf{q},B}(\tau) = \hat{\rho}_{\mathbf{q},B}(\tau) - \langle \hat{\rho}_{\mathbf{q},B}(\tau) \rangle_B$ is the density fluctuation of the electrons. Because of the plasma environment in equilibrium, the condition $\langle \hat{\rho}_{\mathbf{q},B}(\tau) \rangle_B = e_e n_{\text{pl}} \delta_{\mathbf{q},0}$ holds for all time. Then the DSF can be rewritten as

$$S_B(\mathbf{q}, \omega) = \frac{1}{2\pi n_{\text{pl}} \Omega_0 e_e^2} \int_{-\infty}^{\infty} d\tau e^{i\omega\tau} \langle \delta \hat{\rho}_{\mathbf{q},B}(\tau) \delta \hat{\rho}_{-\mathbf{q},B}(0) \rangle_B = \frac{1}{2\pi n_{\text{pl}} \Omega_0} I(-\mathbf{q}, \omega) + \frac{n_{\text{pl}}}{2\pi \Omega_0} \delta(\omega) \delta(\mathbf{q}). \quad (\text{A7})$$

The last term in the above expression contributes only at $\omega = 0$ and $\mathbf{q} = 0$. For dynamical processes this contribution can be neglected.

It can be obviously seen that the functions $\gamma_r(\mathbf{q}, \omega)$, $S_r(\mathbf{q}, \omega)$, $I(\mathbf{q}, \omega)$ and $S_B(\mathbf{q}, \omega)$ are all related to the density-density correlation function and connected to each other, which means that we need only one of them to construct the correlation function of the plasma environment. In this work we use the DSF $S_B(\mathbf{q}, \omega)$ which is directly related to the inverse dielectric function $\epsilon^{-1}(\mathbf{q}, \omega)$ in plasma physics by employing the well-known fluctuation-dissipation theorem [60]:

$$S_B(\mathbf{q}, \omega) = \frac{\hbar}{\pi n_{\text{pl}}} \frac{1}{e^{\hbar\omega/k_B T} - 1} \frac{\epsilon_0 q^2}{e_e^2} \text{Im} \left\{ \lim_{\delta \rightarrow 0^+} \epsilon^{-1}(\mathbf{q}, \omega + i\delta) \right\}. \quad (\text{A8})$$

The dielectric function can be treated by perturbation theory or numerical simulations as a quantum many-body problem. An analytical approach calculating the dielectric function in context of the linear response theory and the random phase approximation can be found, e.g., in Refs. [39, 60].

Appendix B: Rotating Wave Approximation

In this appendix we will investigate the influence of the RWA on the dynamics of the reduced system. The neglect of quickly oscillating terms in Eq. (32) modifies the dynamics of the system. This procedure depends on the choice of the basis $|\psi_n\rangle$ which defines the diagonal and non-diagonal elements of the density matrix.

In contrast to the expressions given in subsec. II C 1, we here consider the result if performing the RWA in an earlier stage. The starting point is the QME (13) (interaction picture) with the influence function (28). The RWA implies that the explicit dependence on $t - t_0$ disappears so that in Eq. (28) only the terms with $m = n'$ and $m' = n$ contribute. We find

$$\hat{\mathcal{D}}_{(1)}^I(t, t_0) = - \sum_{nn', \mathbf{q}} K_{n'n; n'n}(\mathbf{q}, \omega_{n'n}) \left\{ \hat{T}_{n'n'} \hat{\rho}_A^I(t, t_0) - \hat{T}_{nn'} \hat{\rho}_A^I(t, t_0) \hat{T}_{n'n} \right\} + \text{h.c.} \quad (\text{B1})$$

In addition the explicit dependence on $t - t_0$ disappears for $n' = n$ and $m' = m$ so that

$$\hat{\mathcal{D}}_{(2)}^I(t, t_0) = - \sum_{mn, \mathbf{q}} K_{mm; nn}(\mathbf{q}, \omega_{mm}) \left\{ \hat{T}_{mm} \hat{\rho}_A^I(t, t_0) \delta_{mn} - \hat{T}_{mm} \hat{\rho}_A^I(t, t_0) \hat{T}_{nn} \right\} + \text{h.c.} \quad (\text{B2})$$

The term $m = n$ in the sum of $\hat{\mathcal{D}}_{(2)}^I$ gives the same contribution as in $\hat{\mathcal{D}}_{(1)}^I$ if $n' = n$. To avoid this double counting, the corresponding contributions in $\hat{\mathcal{D}}_{(2)}^I$ should be subtracted. The correct contribution can be expressed as

$$\begin{aligned} \hat{\mathcal{D}}_{(2)}^I(t, t_0) &= \sum_{n' \neq n, \mathbf{q}} V_{\mathbf{q}}^2 F_{nn}(\mathbf{q}) F_{n'n'}^*(\mathbf{q}) \left(\Gamma_r(\mathbf{q}, \omega_{n'n'}) + \Gamma_r^*(\mathbf{q}, \omega_{n'n'}) \right) \cdot \hat{T}_{n'n'} \hat{\rho}_A^I(t, t_0) \hat{T}_{nn} \\ &= \sum_{n' \neq n, \mathbf{q}} V_{\mathbf{q}}^2 F_{nn}(\mathbf{q}) F_{n'n'}^*(\mathbf{q}) \gamma_r(\mathbf{q}, 0) \cdot \hat{T}_{n'n'} \hat{\rho}_A^I(t, t_0) \hat{T}_{nn}. \end{aligned} \quad (\text{B3})$$

In dipole approximation, this expression yields no contribution. Beyond dipole approximation this term contributes only to the vertex correction. Altogether, the influence function in RWA follows as

$$\hat{\mathcal{D}}_{\text{RWA}}^I(t, t_0) = \hat{\mathcal{D}}_{(1)}^I(t, t_0) + \hat{\mathcal{D}}_{(2)}^I(t, t_0). \quad (\text{B4})$$

The influence function $\hat{\mathcal{D}}_{(1)}^I(t, t_0)$ can be transformed into a more transparent form. With the decomposition of the response function $\Gamma_r(\mathbf{k}, \omega)$ (20), the influence function (B1) and (B2) can be rewritten as

$$\begin{aligned} \hat{\mathcal{D}}_{(1)}^I(t, t_0) &= - \sum_{nn', \mathbf{q}} \left\{ \frac{1}{2} k_{n'n}(\mathbf{q}, \omega_{n'n}) \left[\{ \hat{T}_{n'n'} \hat{\rho}_A^I(t, t_0) + \hat{\rho}_A^I(t, t_0) \hat{T}_{n'n'} \} - 2 \hat{T}_{nn'} \hat{\rho}_A^I(t, t_0) \hat{T}_{n'n} \right] \right. \\ &\quad \left. - i \sum_{nn', \mathbf{q}} V_{\mathbf{q}}^2 F_{n'n}(\mathbf{q}) F_{nn'}(-\mathbf{q}) S_r(\mathbf{q}, \omega_{n'n}) \left[\hat{T}_{n'n'} \hat{\rho}_A^I(t, t_0) - \hat{\rho}_A^I(t, t_0) \hat{T}_{n'n'} \right] \right\}. \end{aligned} \quad (\text{B5})$$

The last term in Eq. (B5) can be rewritten as commutator describing the reversible Hamiltonian dynamics which in fact represents the line shift of the eigenenergy levels of the atomic system induced by the coupling to the background as known from the coupling to the radiation field. The terms in the first line of the influence function (B5) are responsible for the transition processes of atoms. Since $F_{nn}(\mathbf{q}) F_{n'n'}^*(\mathbf{q})$ is a complex quantity, the influence function $\hat{\mathcal{D}}_{(2)}^I(t, t_0)$ can be also decomposed into a real part

$$\hat{\mathcal{D}}_{(2)}[\hat{\rho}_A(t)] = \sum_{n' \neq n, \mathbf{q}} V_{\mathbf{q}}^2 \cdot \text{Re} \left\{ F_{nn}(\mathbf{q}) F_{n'n'}^*(\mathbf{q}) \right\} \cdot \gamma_r(\mathbf{q}, 0) \cdot \hat{T}_{n'n'} \hat{\rho}_A^I(t, t_0) \hat{T}_{nn} \quad (\text{B6})$$

and an imaginary part

$$\hat{H}_{\text{shift}}^{(2)} = \sum_{n' \neq n, \mathbf{q}} V_{\mathbf{q}}^2 \cdot \text{Im} \left\{ F_{nn}(\mathbf{q}) F_{n'n'}^*(\mathbf{q}) \right\} \cdot \gamma_r(\mathbf{q}, 0) \cdot \hat{T}_{n'n'} \hat{\rho}_A^I(t, t_0) \hat{T}_{nn}. \quad (\text{B7})$$

We go back to the Schrödinger picture with Eq. (12), $\hat{\rho}_A^I(t, t_0) = e^{i(\hat{H}_A + \hat{H}_B)(t-t_0)/\hbar} \hat{\rho}_A(t) e^{-i(\hat{H}_A + \hat{H}_B)(t-t_0)/\hbar}$. Then the atomic QME becomes

$$\frac{\partial \hat{\rho}_A(t)}{\partial t} - \frac{1}{i\hbar} \left[\hat{H}_A + \hat{H}_{\text{shift}}^{(1)} + \hat{H}_{\text{shift}}^{(2)}, \hat{\rho}_A(t) \right] = \hat{\mathcal{D}}_{(1)}[\hat{\rho}_A(t)] + \hat{\mathcal{D}}_{(2)}[\hat{\rho}_A(t)] \quad (\text{B8})$$

with the shift Hamiltonian operator

$$\hat{H}_{\text{shift}}^{(1)} = \sum_{nn', \mathbf{q}} V_{\mathbf{q}}^2 |F_{n'n}(\mathbf{q})|^2 S_r(\mathbf{q}, \omega_{n'n}) \hat{T}_{n'n'}, \quad (\text{B9})$$

which is related the shift of the eigenenergies. The dissipator $\hat{D}_{(1)}[\hat{\rho}_A(t)]$, which is the real part of the influence function is given in Schrödinger picture by

$$\hat{D}_{(1)}[\hat{\rho}_A(t)] = \sum_{nn', \mathbf{q}} k_{n'n}(\mathbf{q}, \omega_{n'n}) \left[\hat{T}_{nn'} \hat{\rho}_A(t) \hat{T}_{n'n} - \frac{1}{2} \left\{ \hat{T}_{n'n'}, \hat{\rho}_A(t) \right\}_+ \right], \quad (\text{B10})$$

where the curly brackets denote the anticommutator. Without the contributions from $\hat{\mathcal{D}}_{(2)}^I[\hat{\rho}_A(t)]$, the QME (B8) has the Lindblad form. Generally, by performing the RWA here we can render the QME in the Lindblad form in which the terms describing atomic emissions and absorptions can be separated as shown in Ref. [38]. However, we should point out that the neglecting of the term $\hat{\mathcal{D}}_{(2)}^I[\hat{\rho}_A(t)]$ yields an incorrect description of the dissipative system beyond dipole approximation.

We implement the matrix representation of the QME (B8) in the Schrödinger picture with Eq. (12), then the atomic QME in RWA becomes

$$\frac{\partial \rho_{A,if}(t)}{\partial t} + i\omega_{if} \rho_{A,if}(t) \quad (\text{B11})$$

$$= - \sum_{n, \mathbf{q}} \left[K_{in;in}(\mathbf{q}, \omega_{in}) + K_{fn;fn}^*(\mathbf{q}, \omega_{fn}) \right] \cdot \rho_{A,if}(t) \\ + \delta_{if} \sum_{n, \mathbf{q}} \left[K_{ni;ni}(\mathbf{q}, \omega_{ni}) + K_{ni;ni}^*(\mathbf{q}, \omega_{ni}) \right] \cdot \rho_{A,nn}(t) \quad (\text{B12})$$

$$+ (1 - \delta_{if}) \sum_{\mathbf{q}} \left[K_{ii;ff}(\mathbf{q}, \omega_{ii}) + K_{ff;ii}^*(\mathbf{q}, \omega_{ff}) \right] \cdot \rho_{A,if}(t). \quad (\text{B13})$$

The last contribution comes from $\hat{\mathcal{D}}_{(2)}^I(t, t_0)$, Eq. (B3).

On the other hand, we can also study the dissipator (B10) in its matrix representation. The Pauli equation resulting from the diagonal matrix elements of the the dissipator (B10) is given by

$$\frac{\partial P_i^{(1)}(t)}{\partial t} = \sum_{n, \mathbf{q}} \left\{ k_{ni}(\mathbf{q}, \omega_{ni}) P_n^{(1)}(t) - k_{in}(\mathbf{q}, \omega_{in}) P_i^{(1)}(t) \right\}. \quad (\text{B14})$$

This relation coincides with the Pauli equation (33) because the contribution $\hat{\mathcal{D}}_{(2)}^I(t, t_0)$ does not affect the behavior of the population numbers given by the diagonal terms of the density matrix. Note that in comparison to the derivation given in this appendix two additional terms occur in Eq. (32), which contain nondiagonal matrix elements $\rho_{A,if}(t)$. The neglecting of these additional terms is only valid if the differences of neighbored eigenenergies E_n of the basis $|\psi_n\rangle$ are enough large so that these terms oscillate quite quickly. In the case of Rydberg states, these terms oscillating with frequency ω_{if} are also relevant and cannot be ignored any more.

The nondiagonal matrix elements of the dissipator (B8), i.e. $\hat{D}_{\text{RWA}}[\hat{\rho}_A(t)] = \hat{D}_{(1)}[\hat{\rho}_A(t)] + \hat{D}_{(2)}[\hat{\rho}_A(t)]$, can be represented as

$$\frac{\partial \rho_{A,if}(t)}{\partial t} + i\tilde{\omega}_{if} \rho_{A,if}(t) = \langle \psi_i | \hat{D}_{\text{RWA}}[\hat{\rho}_A(t)] | \psi_f \rangle = -\frac{1}{2} \left\{ d_1 + d_2 + d_3 \right\} \rho_{A,if}(t) \quad (\text{B15})$$

with the modified transition frequency $\tilde{\omega}_{if}$ due to the shift Hamiltonian in Eq. (B8). The contributions d_1 , d_2 and d_3 are defined similarly as in Eq. (67),

$$d_1 = \sum_{\mathbf{q}} V_{\mathbf{q}}^2 |F_{ii}(\mathbf{q}) - F_{ff}(-\mathbf{q})|^2 \gamma_r(\mathbf{q}, 0), \quad (\text{B16})$$

$$d_2 = \sum_{\mathbf{q}} \{ k_{if}(\mathbf{q}, \omega_{if}) + k_{fi}(\mathbf{q}, \omega_{fi}) \}, \quad (\text{B17})$$

$$d_3 = \sum_{n \neq i, f} \sum_{\mathbf{q}} \{ k_{in}(\mathbf{q}, \omega_{in}) + k_{fn}(\mathbf{q}, \omega_{fn}) \}. \quad (\text{B18})$$

The mixed contribution in d_1 originates from the dissipator $\hat{D}_{(2)}[\hat{\rho}_A(t)]$ (B6), whereas another two contributions belong to the dissipator $\hat{D}_{(1)}[\hat{\rho}_A(t)]$ (B10). It can be seen that the expression (B17) relates directly to the transition rates of the atomic eigenstates comparing with the Pauli equation (33) for a given two-levels system transition, which gives a clue to define the transition rates for the Rydberg wave packet via the QME as explained in Sec. III B.

For the sake of investigating the effect of the RWA we return to the atomic QME (30) which reads in the Schrödinger picture

$$\frac{\partial \rho_{A,if}(t)}{\partial t} + i\omega_{if}\rho_{A,if}(t) = \langle \psi_i | \hat{D}[\hat{\rho}_A(t)] | \psi_f \rangle \quad (\text{B19})$$

with the influence function [remember $\rho_{A,mn}^I(t, t_0) = e^{i\omega_{mn}(t-t_0)}\rho_{A,mn}(t)$]

$$\begin{aligned} \langle \psi_i | \hat{D}[\hat{\rho}_A(t)] | \psi_f \rangle = & - \sum_{mn, \mathbf{q}} \left\{ K_{mn;in}(\mathbf{q}, \omega_{mn}) \rho_{A,mf}(t) + K_{mn;fn}^*(\mathbf{q}, \omega_{mn}) \rho_{A,im}(t) \right. \\ & \left. - [K_{mi;fn}(\mathbf{q}, \omega_{mi}) + K_{nf;mi}^*(\mathbf{q}, \omega_{nf})] \rho_{A,mn}(t) \right\}. \end{aligned} \quad (\text{B20})$$

The RWA for the non-diagonal terms means we should set $m = i$ in the first term, $m = f$ in the second term and $m = i$, $n = f$ in the third term of the influence function (B20). By using the decomposition of the complex response function $\Gamma_r(\mathbf{q}, \omega) = \gamma_r(\mathbf{q}, \omega)/2 + iS_r(\mathbf{q}, \omega)$ we obtain the same expression as Eq. (B15).

In principle, the RWA by the removal of terms that oscillate quickly with respect to some characteristic time scales of the system yields is problematic as pointed out by different authors. It depends on the choice of the basis $|\psi_n\rangle$ for the representation of the density matrix, and in the case of small energy differences of neighbored eigenenergies E_n the oscillation may become not quick enough compared to the characteristic time scales of the system. Also recently the RWA is under discussion. In a study of the spontaneous emission of a two-level system, Agarwal found that the RWA gives an incorrect value for environmentally induced frequency shifts with respect to the system frequency [63]. Fleischhauer studied the photodetection without the RWA, finding that for ultrashort pulses, whose length is of the order of the oscillation period, the mean number of photocounts with the RWA and without the RWA are substantially different [64]. Recently, Fleming *et al.* investigated the validity of the RWA in an open quantum system and argued that the quantum state resulting from the RWA is inappropriate for calculating the detailed properties of the state dynamics such as entanglement dynamics [65]. In Ref. [66], Majenz *et al.* showed that the RWA leads to the missing of important qualitative features of the population dynamics in a special three-level model. Recently, Mäkelä and Möttönen [67] discovered that the RWA yields an impressive reduction in the amount of non-Markovianity and is problematic if non-Markovian dynamics is of essential relevance.

In this work, we found that the RWA performed in Eq. (28) by neglecting $\hat{D}_{(2)}^I(t, t_0)$ leads to a QME in Lindblad form. However, the term $\hat{D}_{(2)}^I(t, t_0)$ has a significant contribution in some special cases, for example, the vertex correction of the spectral line profiles. On the other hand, if the RWA is performed in the matrix representation, the contribution of $\hat{D}_{(2)}^I(t, t_0)$ can be automatically included in the influence function. If the RWA is carried out prematurely, it will be inappropriate to describe the dissipative properties of the relevant atomic system (Rydberg states) and result in erroneous transition rates.

Appendix C: Derivation of the QME for the Spectral Profile

As mentioned before, the charge density operator in the case of spectral line profiles is given by

$$\hat{\rho}_{\mathbf{q},S}^I(\omega) = \sum_{n'>n} e_e \hat{T}_{n'n}^- \cdot F_{n'n}(\mathbf{q}) \delta(\omega - \Delta\omega_{n'n}) - \sum_{n'<n} e_e \hat{T}_{n'n}^+ \cdot F_{n'n}(\mathbf{q}) \delta(\omega + \Delta\omega_{nn'}). \quad (\text{C1})$$

The first term in (C1) describes the absorption process which the second one signifies the emission process. Inserting this expression into the influence function (21), we obtain a new influence function including both emission and absorption terms, which can be used as the starting point to derive the spectral line profile. The terms representing the emission processes can be selected by using the matrix element representation $\langle \tilde{f} | \mathcal{D}^I[\hat{\rho}_S(t)] | \tilde{i} \rangle$ with the change of the photon number $\Delta N = N_f(\tilde{\mathbf{k}}) - N_i(\tilde{\mathbf{k}}) = 1$:

$$\langle \tilde{f} | \mathcal{D}^I[\hat{\rho}_S^I(t)] | \tilde{i} \rangle = -A_1 - A_2 + A_3 + A_4 \quad (\text{C2})$$

with

$$\begin{aligned}
A_1 &= \sum_{n>f, m<n, \mathbf{q}} \exp[i(-\Delta\omega_{nm} + \Delta\omega_{nf})t] K_{fn;nm}(\mathbf{q}, \Delta\omega_{nm}) \langle \psi_m, \Delta N | \hat{\rho}_S(t) | \psi_i \rangle \\
&\quad + \sum_{n<f, m>n, \mathbf{q}} \exp[i(\Delta\omega_{mn} - \Delta\omega_{fn})t] K_{fn;nm}(\mathbf{q}, -\Delta\omega_{mn}) \langle \psi_m, \Delta N | \hat{\rho}_S(t) | \psi_i \rangle, \\
A_2 &= \sum_{n>i, m<n, \mathbf{q}} \exp[-i(-\Delta\omega_{nm} + \Delta\omega_{ni})t] K_{mn;ni}^*(\mathbf{q}, \Delta\omega_{nm}) \langle \psi_f, \Delta N | \hat{\rho}_S(t) | \psi_m \rangle \\
&\quad + \sum_{n<i, m>n, \mathbf{q}} \exp[-i(\Delta\omega_{mn} - \Delta\omega_{in})t] K_{mn;ni}^*(\mathbf{q}, \Delta\omega_{nm}) \langle \psi_f, \Delta N | \hat{\rho}_S(t) | \psi_m \rangle, \\
A_3 &= \sum_{i>n, m<f, \mathbf{q}} \exp[i(-\Delta\omega_{fm} + \Delta\omega_{in})t] \{ K_{ni;fm}(\mathbf{q}, \Delta\omega_{fm}) + K_{mf;in}^*(\mathbf{q}, \Delta\omega_{in}) \} \langle \psi_m, \Delta N | \hat{\rho}_S(t) | \psi_n \rangle, \\
A_4 &= \sum_{i<n, m>f, \mathbf{q}} \exp[i(-\Delta\omega_{fm} + \Delta\omega_{in})t] \{ K_{ni;fm}(\mathbf{q}, -\Delta\omega_{mf}) + K_{mf;in}^*(\mathbf{q}, -\Delta\omega_{ni}) \} \langle \psi_m, \Delta N | \hat{\rho}_S(t) | \psi_n \rangle,
\end{aligned}$$

where the indexes m and n are interchanged. These terms can be further simplified in RWA. This means that we can set $m = f$ in A_1 , $m = i$ in A_2 , and $m = f$, $n = i$ in A_3 and A_4 . The QME in RWA becomes

$$\frac{\partial \rho_{S,fi}^I(t)}{\partial t} = -\Gamma_{fi}^{BS}(\omega_{\mathbf{k}}) \rho_{S,fi}^I(t) + \Gamma_{fi}^\nu \rho_{S,fi}^I(t) \quad (\text{C3})$$

with a coefficient $\Gamma_{fi}^{BS}(\omega_{\mathbf{k}})$ describing the shift of the eigenenergy levels and the pressure broadening

$$\Gamma_{fi}^{BS}(\omega_{\mathbf{k}}) = \sum_{n, \mathbf{q}} \{ K_{nf;fn}(\mathbf{q}, \Delta\omega_{nf}) + K_{nf;fn}(\mathbf{q}, -\Delta\omega_{fn}) + K_{ni;in}^*(\mathbf{q}, \Delta\omega_{ni}) + K_{ni;in}^*(\mathbf{q}, -\Delta\omega_{in}) \} \quad (\text{C4})$$

and a coefficient Γ_{fi}^V describing the vertex correction

$$\Gamma_{fi}^V = \sum_{\mathbf{q}} \{ K_{ii;ff}(\mathbf{q}, \Delta\omega_{ff}) + K_{ii;ff}(\mathbf{q}, -\Delta\omega_{ff}) + K_{ff;ii}^*(\mathbf{q}, \Delta\omega_{ii}) + K_{ff;ii}^*(\mathbf{q}, -\Delta\omega_{ii}) \}, \quad (\text{C5})$$

which has no dependence on $\omega_{\mathbf{k}}$ in our approximation.

Appendix D: Collisional Decoherence of a Rydberg Electron in Plasma

Following the method represented in the book of Joos *et al.* [2] the reduced density matrix for the Rydberg electron can be derived under the assumptions of recoil-free collisions and elastic scattering

$$\rho(\mathbf{R}_n, \mathbf{R}'_n) \rightarrow \rho(\mathbf{R}_n, \mathbf{R}'_n) \cdot \left\{ 1 + \sum_{\mathbf{k}'} \left[1 - e^{i(\mathbf{k}-\mathbf{k}') \cdot (\mathbf{R}_n - \mathbf{R}'_n)} \right] |\langle \mathbf{k}', n | \hat{T} | \mathbf{k}, n \rangle|^2 \right\}, \quad (\text{D1})$$

where the T-matrix is given by $\hat{T} = \hat{V} + \hat{V} \hat{G}_0 \hat{V} + \hat{V} \hat{G}_0 \hat{V} \hat{G}_0 \hat{V} + \dots$. In the elastic scattering process the principal quantum number n of the Rydberg electron does not change, this means, the Rydberg electron motions along the classical Kepler orbit. For the bound electrons the T-matrix in Born approximation can be represented as

$$\langle \mathbf{k}', n | \hat{T} | \mathbf{k}, n \rangle = V_{\mathbf{q}} F_{nn}(\mathbf{q}) \delta(E_{\mathbf{k}} - E_{\mathbf{k}'}), \quad (\text{D2})$$

with $\mathbf{q} = \mathbf{k} - \mathbf{k}'$ and $E_{\mathbf{k}} = \mathbf{k}^2/(2m_e)$. $V_{\mathbf{q}}$ denotes the interaction potential and $F_{nn}(\mathbf{q})$ is diagonal atomic form factor.

In Born approximation we have

$$\begin{aligned}
A &:= \sum_{\mathbf{k}'} \left[1 - e^{i(\mathbf{k}-\mathbf{k}') \cdot (\mathbf{R}_n - \mathbf{R}'_n)} \right] |\langle \mathbf{k}', n | \hat{T} | \mathbf{k}, n \rangle|^2 \\
&= \frac{\Omega_0}{(2\pi)^3} \int d^3 \mathbf{k}' \left[1 - e^{i(\mathbf{k}-\mathbf{k}') \cdot (\mathbf{R}_n - \mathbf{R}'_n)} \right] V_{\mathbf{q}}^2 F_{nn}^2(\mathbf{q}) \delta^2(E_{\mathbf{k}} - E_{\mathbf{k}'}) \\
&= \frac{\Omega_0 m_e T}{(2\pi \hbar)^3 k} \int_0^{2k} dq q V_{\mathbf{q}}^2 F_{nn}^2(\mathbf{q}) \left[1 - e^{i\mathbf{q} \cdot (\mathbf{R}_n - \mathbf{R}'_n)} \right].
\end{aligned} \quad (\text{D3})$$

In the third line the integrals over k' and ϕ have been carried out and the integral over θ is replaced by $\int_{|k-k'|}^{k+k'} dq$ by using the relation $q^2 = k^2 + k'^2 - 2kk' \cos \theta$. The squared delta function is evaluated by using the Fourier representation of the delta function

$$\delta^2(E_{\mathbf{k}} - E_{\mathbf{k}'}) = \delta(E_{\mathbf{k}} - E_{\mathbf{k}'}) \cdot \lim_{T \rightarrow \infty} \frac{1}{2\pi\hbar} \int_{-T/2}^{T/2} dt e^{i(E_{\mathbf{k}} - E_{\mathbf{k}'})t/\hbar} = \frac{m_e}{\hbar^2 k'} \delta(k - k') \cdot \lim_{T \rightarrow \infty} \frac{T}{2\pi\hbar}. \quad (\text{D4})$$

For a collection of N independent scattering events in plasma, the above expression (D3) should be multiplied by a factor N . For the momentum distribution $P(\mathbf{q})$ of the plasma environment, the classical Maxwell-Boltzmann distribution is taken, where the momentum distribution $P(\hbar\mathbf{k})$ of the plasma environment, assumed to fulfill Maxwell-Boltzmann distribution $P(\mathbf{q}) = (\frac{\hbar^2}{2\pi m_e k_B T})^{3/2} \exp[-\hbar^2 q^2 / (2m_e k_B T)]$ is taken. We find

$$A = \frac{N\Omega_0 T}{\pi(2\pi\hbar)^2} \sqrt{\frac{m_e}{2\pi k_B T}} \int_0^\infty dq q V_{\mathbf{q}}^2 F_{nn}^2(\mathbf{q}) e^{-\hbar^2 q^2 / (8m_e k_B T)} \left[1 - e^{i\mathbf{q} \cdot (\mathbf{R}_n - \mathbf{R}'_n)}\right]. \quad (\text{D5})$$

For the scattering process described here we have the time evolution of the reduced density matrix (QME) by taking the differential limit of small T

$$\frac{\rho(\mathbf{R}_n, \mathbf{R}'_n, T) - \rho(\mathbf{R}_n, \mathbf{R}'_n, 0)}{T} = \frac{N\Omega_0}{\pi(2\pi\hbar)^2} \sqrt{\frac{m_e}{2\pi k_B T}} \int_0^\infty dq q V_{\mathbf{q}}^2 F_{nn}^2(\mathbf{q}) e^{-\hbar^2 q^2 / (8m_e k_B T)} \left[1 - e^{i\mathbf{q} \cdot (\mathbf{R}_n - \mathbf{R}'_n)}\right]. \quad (\text{D6})$$

To avoid the divergence of the integral in (D6), the Debye potential [60] can be used. As the next step we can use the long-wavelength limit to evaluate (D6), i.e. we can expand the exponential function $e^{i\mathbf{q} \cdot (\mathbf{R}_n - \mathbf{R}'_n)}$ up to second order and obtain the QME in the long-wavelength limit

$$\frac{\partial}{\partial t} \rho(\mathbf{R}_n, \mathbf{R}'_n, t) = -\frac{N\Omega_0}{\pi(2\pi\hbar)^2} \sqrt{\frac{m_e}{2\pi k_B T}} \int_0^\infty dq q V_{\mathbf{q}}^2 F_{nn}^2(\mathbf{q}) e^{-\hbar^2 q^2 / (8m_e k_B T)} (\mathbf{q} \cdot (\mathbf{R}_n - \mathbf{R}'_n))^2. \quad (\text{D7})$$

As shown in Sec. III A, the Rydberg electron moves along the Kepler orbit, i.e. $\mathbf{R}_n = (n^2 a_B, \pi/2, \phi)$ and $\mathbf{R}'_n = (n^2 a_B, \pi/2, \phi')$. This assumption allows us to calculate the term $(\mathbf{q} \cdot (\mathbf{R}_n - \mathbf{R}'_n))^2$ by averaging it over all possible directions $(\mathbf{R}_n - \mathbf{R}'_n)$: $(\mathbf{q} \cdot (\mathbf{R}_n - \mathbf{R}'_n))^2 = q^2 \cdot (x - x')^2 / 3$ with $x = r_{\text{cl}} \phi$. Then we have

$$\frac{\partial}{\partial t} \rho(x, x', t) = -\Lambda_{R_n} \cdot (x - x')^2 \quad (\text{D8})$$

with the localization rate defined by

$$\Lambda_{R_n} = \frac{N\Omega_0}{\pi(2\pi\hbar)^2} \int_0^\infty dq \frac{q^4}{3} V_{\mathbf{q}}^2 F_{nn}^2(\mathbf{q}) \sqrt{\frac{m_e}{2\pi k_B T q^2}} e^{-\hbar^2 q^2 / (8m_e k_B T)}. \quad (\text{D9})$$

For a free electron moving in the plasma environment we can recover the localization rate from the expression (D9) by setting $F_{nn}^2(\mathbf{q}) = 1$, which coincides with the result reported in Ref. [61] up to a factor $2\pi^2$.

Bib

-
- [1] M. Schlosshauer, *Decoherence and the Quantum-To-Classical Transition* (Springer, Berlin, 2007).
 - [2] E. Joos, H.D. Zeh, C. Kiefer, D. Giulini, J. Kupsch, and I.O. Stamatescu, *Decoherence and the Appearance of a Classical World in Quantum Theory* (Springer, Berlin, 2003).
 - [3] Y. N. Gnedin *et al.*, New Astronomy Reviews **53**, 259 (2009).
 - [4] D. Vranceanu, R. Onofrio, and H. R. Sadeghpour, ApJ **780**, 2 (2014).
 - [5] A. A. Mihajlov *et al.*, Phys. Scr. **53**, 159 (1996).
 - [6] A. A. Mihajlov *et al.*, Phys. Scr. **56**, 631 (1997).
 - [7] W. Ebeling, W.-D. Kraeft, D. Kremp and G. Röpke, ApJ **290**, 24 (1985).
 - [8] B. Omar *et al.*, Contrib. Plasma Phys. **47**, 315 (2007).
 - [9] B. Omar *et al.*, Contrib. Plasma Phys. **51**, 22 (2011).

- [10] M. Saffman, T. G. Walker, and K. Mølmer, *Rev. Mod. Phys.* **82**, 2313 (2010).
- [11] H. Labuhn, S. Ravets, D. Barredo, L. Béguin, F. Nogrette, T. Lahaye, and A. Browaeys, *Phys. Rev. A* **90**, 023415 (2014).
- [12] S. Ravets, H. Labuhn, D. Barredo, L. Béguin, T. Lahaye, and A. Browaeys, *Nat. Phys.* **10**, 914 (2014).
- [13] N. Vanhaecke, D. Comparat, D. A. Tate, and P. Pillet, *Phys. Rev. A* **71**, 013416 (2005).
- [14] T.C. Killian, T. Pattard, T. Pohl, and J.M. Rost, *Physics Reports* **449**, 77 (2007).
- [15] G. Ranjit and C. I. Sukenik, *Phys. Rev. A* **87**, 033418 (2013).
- [16] T. Kazimierczuk, D. Fröhlich, S. Scheel, H. Stolz, and M. Bayer, *Nature* **514**, 343 (2014).
- [17] P. Grünwald, M. Aßmann, D. Fröhlich, M. Bayer, H. Stolz, and S. Scheel, *arXiv:1511.07742* (2015).
- [18] E. Schrödinger, *Naturwissenschaften* **14**, 664 (1926).
- [19] C. G. Darwin, *Proc. Roy. Soc. A* **117**, 258 (1928).
- [20] J. Parker and C. R. Stroud Jr, *Phys. Rev. Lett.* **56**, 716 (1986).
- [21] J. A. Yeazell, M. Mallalieu, J. Parker, and C. R. Stroud Jr, *Phys. Rev. A* **40**, 5040 (1989).
- [22] J. A. Yeazell, M. Mallalieu, and C. R. Stroud Jr, *Phys. Rev. Lett.* **64**, 2007 (1990).
- [23] J. A. Yeazell and C. R. Stroud Jr, *Phys. Rev. A* **43**, 5153 (1991).
- [24] M. Mallalieu and C.R. Stroud Jr, *Phys. Rev. A* **49**, 2329 (1994).
- [25] M. W. Noel and C. R. Stroud Jr, *Phys. Rev. Lett.* **77**, 1913 (1996).
- [26] P. Bellomo *et al.*, *Phys. Rev. A* **58**, 3896 (1998).
- [27] J. Bromage and C. R. Stroud, *Phys. Rev. Lett.* **83**, 4963 (1999).
- [28] C. Gocke and G. Röpke, *J. Phys. A: Math. Gen.* **39**, 4587 (2006).
- [29] C. Gocke and G. Röpke, *Contrib. Plasma Phys.* **47**, 291 (2007).
- [30] C. Gocke and G. Röpke, *Theoretical and Mathematical Physics* **154**, 26 (2008).
- [31] B. Vacchini and K. Hornberger, *Phys. Rep.* **478**, 71 (2009).
- [32] A. Smirne and B. Vacchini, *Phys. Rev. A* **82**, 042111 (2010).
- [33] E. W. Smith, J. Cooper, and C. R. Vidal, *Phys. Rev.* **185**, 140 (1969).
- [34] M. Baranger, *Phys. Rev.* **112**, 855 (1958).
- [35] L. Klein, *J. Quant. Spectrosc. Radiat. Transfer* **9**, 199 (1969).
- [36] S. Günter, L. Hitzschke, and G. Röpke, *Phys. Rev. A* **44**, 6834 (1991).
- [37] H. Reinholz, *Ann. Phys. Fr.* **30**, 1 (2005).
- [38] H. P. Breuer and F. Petruccione, *The Theory of Open Quantum Systems* (Clarendon Press, Oxford, 2007).
- [39] G. Röpke, *Nonequilibrium Statistical Physics* (WILEY-VCH, Weinheim, 2013).
- [40] J. Bretón, A. Hardisson, F. Mauricio, and S. Velasco, *Phys. Rev. A* **30**, 553 (1984).
- [41] D. N. Zubarev, W. Morosov and G. Röpke, *Statistical Mechanics of Nonequilibrium Processes* (Akademie-Verlag, Berlin, 1997).
- [42] A. Könies and S. Günter, *Phys. Rev. E* **52**, 6658 (1995).
- [43] R. J. Glauber, *Phys. Rev.* **131**, 2766 (1963).
- [44] L. S. Brown, *Am. J. Phys.* **41**, 525 (1973).
- [45] M. M. Nieto and L. M. Simmons, *Phys. Rev. Lett.* **41**, 207 (1978).
- [46] D. Bhaumik, B. Dutta-Roy, and G. Ghosh, *J. Phys. A* **19**, 1355 (1986).
- [47] I. Zaltev, W. M. Zhang, and D. H. Feng, *Phys. Rev. A* **50**, R1973 (1994).
- [48] P. Majumdar and H. S. Sharatchandra, *Phys. Rev. A* **56**, R3322 (1997).
- [49] A. J. Makowski and P. Pełowski, *Phys. Rev. A* **86**, 042117 (2012).
- [50] A. J. Makowski and P. Pełowski, *Ann. Phys.* **337**, 25 (2013).
- [51] Z. D. Gaeta and C. R. Stroud Jr, *Phys. Rev. A* **42**, 6308 (1990).
- [52] R.W. Robinett, *Phys. Rep.* **392**, 1 (2004).
- [53] J. R. Klauder, *J. Phys. A* **29**, L293 (1996).
- [54] R. F. Fox, *Phys. Rev. A* **59**, 3241 (1999).
- [55] P. Mansbach and J. Keck, *Phys. Rev.* **181**, 275 (1969).
- [56] L. Vriens and A. H. M. Smeets, *Phys. Rev. A* **22**, 940 (1980).
- [57] F. Devos, J. Boulmer and J.-F. Delpèch, *J. Phys. (Paris)* **40**, 215 (1979).
- [58] I. L. Beigman and V. S. Lebedev, *Phys. Rep.* **250**, 9528 (1995).
- [59] J.P. Hansen and I.R. McDonald, *Theory of Simple Liquids* (Academic Press, London, 1986).
- [60] D. Kremp, M. Schlanges, W.-D. Kraeft, *Quantum Statistics of Nonideal Plasmas* (Springer, Berlin, 2005).
- [61] B. Vacchini, Test particle in a quantum gas. *Phys. Rev. E* **63**, 066115 (2001).
- [62] D. Salzmann, *Atomic Physics in Hot Plasmas* (Oxford University Press, New York, 1998).
- [63] G. S. Agarwal, *Phys. Rev. A* **4**, 1778 (1971); *Phys. Rev. A* **7**, 1195 (1973).
- [64] M. Fleischhauer, *J. Phys. A: Math. Gen.* **31**, 453 (1998).
- [65] C. Fleming *et al.*, *J. Phys. A: Math. Theor.* **43**, 405304 (2010).
- [66] C. Majenz *et al.*, *Phys. Rev. A* **88**, 012103 (2013).
- [67] H. Mäkelä and M. Möttönen, *Phys. Rev. A* **88**, 052111 (2013).